

BEAM QUALITY SPECIFICATION IN KILO-VOLTAGE RADIOTHERAPY



Sibusiso Jozela

A research report submitted to the Faculty of Science, University of the Witwatersrand, Johannesburg, in partial fulfilment of the requirements for the degree of the Master of Science.

Johannesburg, 2007

DECLARATION

I declare that this research report is my own, unaided work. It is being submitted for the degree of Master of Science in the University of the Witwatersrand, Johannesburg. It has not been submitted before for any degree or examination in any other University.

(Signature of a candidate)

5th day of March 2007

ABSTRACT

Purpose: The purpose of this work was to compare and analyse two clinically measurable beam quality specifiers, the half value layer (HVL) and the ratio of the doses at depths 2 cm and 5 cm (D_2/D_5) for a range of kilovoltage modalities, and to determine whether a practical, alternative and/or better correlation exists.

Methods and materials: Four x-ray units were used: two Philips RT 250 units, a Pantak HF 420 operated up to 250 kV, and a D3300 Gulmay Medical unit operated up to 300 kV. As not all these units were equipped with an internal monitor chamber, a system was used where either the first measurement was repeated at the end of each series or an external monitor chamber was employed in order to ensure output constancy. A range of HVL's were measured on each of the energies investigated on this work, which were used clinically. A calibrated 0.6 cc ionization chamber was used in a 30 cm x 30 cm x 30 cm water phantom to measure the absorbed dose to water at depths 2 cm and 5 cm in order to investigate D_2/D_5 as the alternative quality index.

Results: The effectiveness of using a monitor chamber in the determination of HVL has been shown to be significant in this work where HVLs differed by up to 3%. Errors incurred from using HVL have been identified. This work verified that the ratio of doses at depths 2 cm and 5 cm in water could be applied as a kilovoltage beam quality specifier in the clinical environment at low and medium energies with a well defined FSD and field size.

Conclusions: The use of D_2/D_5 as a tool to verify the beam quality index would simplify quality control in the clinical environment. Further work would have to be done to investigate other energies. Lower energies may require the use of shallower depths in order to improve accuracy and ensure a more clinically relevant setup.

DEDICATION

TO MY MOTHER TOKOZILE DOREEN JOZELA, MY BROTHERS
AND SISTER
AND TO ALL MY FRIENDS FOR THEIR ENCOURAGEMENT

ACKNOWLEDGEMENTS

This research report would not have been possible without the assistance and cooperation of certain individuals and institutions, and the author would particularly like to thank the following:

I would like to sincerely express my gratefulness to my supervisor Professor D. G. van der Merwe for her endless inputs, encouragement and wonderful guidance throughout my entire research and for her wisdom, may God be with her always.

I would also like to thank:

Radiation Oncology department in the Pretoria Academic hospital for allowing me to use the hospital's facilities during my research. CSIR National Metrology Laboratory (NML) and Miss Zakithi Msimang for letting me use their facilities to get more data and her help is much appreciated. Dr K. E. Rosser, for her willingness to respond whenever I needed some clarity, I appreciate all her help.

Table of Contents

DECLARATION	II
ABSTRACT.....	III
DEDICATION.....	IV
ACKNOWLEDGEMENTS.....	V
TABLE OF CONTENTS	VI
LIST OF FIGURES.....	VIII
LIST OF TABLES	X
1. INTRODUCTORY CHAPTER	1
1.1 INTRODUCTION	1
1.1.1 History of x-rays in radiation therapy	1
1.1.2 Current use in era of linear accelerators.....	2
1.1.3 Assessment of need	2
1.2 DOSIMETRY.....	2
1.2.1 Survey of the kilo-voltage radiotherapy centers in the UK.....	4
1.3 NEED FOR THE STUDY	7
1.4 RESEARCH OBJECTIVE	7
2. FACTORS AFFECTING THE QUALITY OF X-RAY BEAMS.....	8
2.1 THE QUALITY OF X-RAYS	8
2.2 EFFECTS OF FILTERS ON AN X-RAY BEAM.....	8
2.3 THE MEASUREMENT OF HALF VALUE LAYER.....	10
2.4 EFFECT OF SCATTER ON HVL MEASUREMENTS	14
2.5 EFFECTS OF DETECTOR ON HVL MEASUREMENT	16
2.6 HVL AND FILTERS FOR THERAPY.....	18
3. CODES OF PRACTICE IN KILOVOLTAGE THERAPY	19
3.1 HISTORICAL REVIEW	19
3.2 EQUIPMENT.....	19
3.2.1 Dosimeters.....	19
3.2.2 Electrometers.....	20

3.2.3 Phantoms	20
3.3 RADIATION QUALITY SPECIFICATION AND DETERMINATION	21
3.4 A SUMMARY OF KILOVOLTAGE CODES OF PRACTICE OVER THE LAST FEW DECADES	22
4. METHODS AND MATERIALS	26
4.1 EQUIPMENT.....	26
4.2 HVL DETERMINATION	27
4.3 MEASUREMENT OF ABSORBED DOSE AT 2 cm AND 5 cm DEPTHS...30	
5. RESULTS AND ANALYSIS	31
5.1 HVL RESULTS.....	31
5.1.1 Significance of a monitor chamber	31
5.2 RELATIONSHIP BETWEEN HVL AND GENERATING POTENTIAL	31
5.2.1 Comparison of clinical and laboratory beam qualities.....	31
5.3 COMPARISON OF HVL AND THE RATIO OF D_2/D_5 AS QUALITY INDEXES	37
5.3.1 HVL as a beam quality index	37
5.3.2 D_2/D_5 as a beam quality index	40
6. DISCUSSION	48
7. CONCLUSIONS	51
APPENDIX A.....	52
A. DOSIMETRIC PRINCIPLES	52
A.1 INTRODUCTION	52
A.2 PHOTON FLUENCE AND ENERGY FLUENCE	52
A.3. KERMA	55
A.3.1 Theoretical basis for the new air kerma based code	55
A.3.2 Medium-energy x-rays (0.5 mm Cu-4 mm Cu).....	56
A.3.3 Low-energy x-ray beams.....	58
A.4 ABSORBED DOSE.....	59
A.5 DETERMINATION OF THE RATIO OF MASS-ENERGY ABSORPTION COEFFICIENT OF WATER TO AIR	60
8 . REFERENCES.....	61

LIST OF FIGURES

Figure 1-1. Variation in the half value layer (HVL) with the generating potential for 26 UK radiotherapy centers at medium energies ⁶	5
Figure 1-2. Variation in the half value layer (HVL) with the generating potential for 26 UK radiotherapy centers at low energies ⁶	6
Figure 2-1. Graph showing how the spectral distribution of radiation generated by 200 keV electrons bombarding a thick tungsten target changes with filtration. Dashed line A, unfiltered beam. Curves B, C, D, and E are obtained from A by calculating the attenuation produced by the indicated layers of Al, Cu, and Sn ⁷ . 9	9
Figure 2-2. An ideal arrangement for accurate measurement of the half value layer (HVL) ⁷	11
Figure 2-3. Experimentally determined attenuation curve for 200 kV radiation, showing how the HVL may be determined for a number of filtrations ⁷	13
Figure 2-4. Diagrams to illustrate how different apparent half value layers may be obtained for the same beam using different arrangements of field size and attenuator position during the measurements ⁷	15
Figure 2-5. Graph showing how the measured attenuation of a beam from a 130 kV x-ray machine depends upon the type of detector used in the experiment ⁷	17
Figure 3-1. Comparison of the value of k_h recommended by the IPEMB, with the original IAEA ³ and the revised IAEA (1993) values across the medium energy range ¹⁴	25
Figure 4-1. The experimental setup for an HVL measurement without a monitor chamber.....	28
Figure 4-2. The experimental setup for an HVL measurement with a monitor chamber.....	29
Figure 5-1. Two determinations of the HVL with the chamber readings corrected and uncorrected against the monitor chamber.....	32
Figure 5-2. The relationship between HVL and generating potential for some SSDL and Codes of Practice at low energies.	33
Figure 5-3. The relationship between HVL and generating potential for SSDL and Codes of Practice at medium energies.....	34
Figure 5-4. The variation of HVL with generating potential for hospital units and the South African SSDL at low energies.....	35

Figure 5-5. The variation of HVL with generating potential for the hospital units and the South African SSDL at medium energies.	36
Figure 5-6. The relationship between the HVL at 100 kV and the MEAC.	38
Figure 5-7. The relationship between the HVL generated at 250 kV and 300 kV and the MEAC.	39
Figure 5-8. The variation in MEAC with D_2/D_5 at an FSD of 100 cm for different HVLs at 100 kV for the Pantak HF 420 unit. The solid line is the linear regression of the data points.	41
Figure 5-9. The variation in MEAC with D_2/D_5 at an FSD of 100 cm for different HVLs at 250 kV for the Pantak HF 420 unit. The solid line is the linear regression of the data points.	42
Figure 5-10. The variation in MEAC with D_2/D_5 at an FSD of 50 cm for different HVLs at 300 kV for the D3300 unit. The solid line is the linear regression of the data points. Measurements were taken at a field size of $10 \times 10 \text{ cm}^2$	43
Figure 5-11. The variation in MEAC with D_2/D_5 as a function of different HVLs at 300 kV for the D3300 Gulmay Medical unit. Measurements were taken at the standard FSD of 50 cm and a range of field sizes are shown.	44
Figure 5-12. D_2/D_5 as a function of HVL at low energies. The solid line is the regression that best fits the data points to the resulting equation given on the graph.	46
Figure 5-13. D_2/D_5 as a function of HVL at medium energies. The solid line is the regression that best fits the data points to the resulting equation given on the graph.	47
Figure A-1. Photon fluence and energy fluence spectra at 1 m from the target of an x-ray machine with a tube potential of 250 kV and added filtration of 1 mm Al and 1.8 mm Cu (target material: W; inherent filtration: 2 mm Be). ⁹	54

LIST OF TABLES

TABLE 3-1 A SUMMARY OF THE DOSIMETRY OF KILOVOLTAGE CODES OF PRACTICE..	22
TABLE 4-1. GEOMETRY USED IN THE RELATIVE DOSE MEASUREMENTS.....	30

1. INTRODUCTORY CHAPTER

1.1 INTRODUCTION

1.1.1 History of x-rays in radiation therapy

X-rays were used in the treatment of various benign and malignant conditions within a year of their discovery. The first reported cure of cancer, a basal cell epithelioma, by this treatment modality appeared in the literature in 1899.¹ During this time it was viewed as the "Dark Ages" in the evolution of radiation therapy as a treatment modality for cancer, with radium used as the source of radiation delivery. Surgeons or dermatologists administered the radiation therapy treatment, with little understanding or knowledge of the physical nature and biological effects of radiation. There was no method of calculating the radiation dosage. The equipment used to deliver the radiation was primitive and temperamental. However it was not until the invention of the hot cathode tube by Coolidge in 1913 that x-ray beams could be delivered in a stable manner and the output controlled and measured with any precision. In those early years, x-ray beams were limited to energies ranging from 80 kV to 140 kV so only relatively superficial lesions could be successfully treated. In the early 1920's, higher energy x-ray units became available to permit the treatment of deep-seated lesions.

Radiation therapy of this era involved a massive exposure of radiation to a large area of the body with the hope that the tumor would be destroyed with a single treatment¹. Needless to say, many complications occurred after treatment with radiation, due to the destruction of the normal tissues. The literature of this decade has many examples of tissue necrosis, infection and death as a result of treatment. The rate of tumor recurrence was also reported as high. This was the era of kilovoltage radiotherapy. With the introduction of the vacuum x-ray tube, capable of energies as high as 200 kV, cures however of superficial cancers were also soon reported. It became clear that machines capable of producing higher energies had to be developed in order to effectively treat cancer located below the surface of the skin.

1.1.2 Current use in era of linear accelerators

Even though high-energy linear accelerators, capable of producing megavoltage electron and photon beams, have largely replaced kilovoltage x-ray units, there seems to be a renewed interest in irradiation of certain superficial lesions with kilovoltage modalities, which remain the preferred approach in certain circumstances. In recent years, there has also been an increase in the use of low-energy x-rays as an intraoperative modality, such as stereotactic brain irradiation, partial breast irradiation or treatment of the dura, for endocavitary irradiation of rectal cancers and treatment of other malignant skin lesions².

1.1.3 Assessment of need

Kilovoltage x-ray machines are used in hospital environments for treating cancer patients. Other important applications of these machines are in dosimetry and radiobiological research, where the requirements from the machine can be quite different from the clinic, e.g., they are usually housed in small enclosures with little or no movement of the x-ray tube².

1.2 DOSIMETRY

The necessity for the specification of radiation beam quality arises from the fact that several parameters required for the determination of absorbed dose, depend on the source energy. Examples of such parameters are calibration factors, mass-energy absorption coefficients, electron stopping powers, and various other perturbation factors. Complete characterization of a radiation beam would involve specification of the type, number of particles, and their energy and angular distribution. This type of information is very difficult to obtain however it has been considered possible to perform clinically acceptable dosimetry with much less detail³. A number of more practical schemes for indirectly specifying the radiation beam quality have therefore been devised, such as the half value layer (HVL). When the spectral distribution of the radiation beam can be significantly varied by the choice of kV and filtration to achieve a particular HVL in aluminum or copper, reference to HVL alone may prove inadequate as the only specification of the beam quality with regard to the percent depth dose (PDD)⁴. In such instances a two-parameter specification such as HVL plus kV or HVL plus homogeneity coefficient (HC) may be more adequate⁴. Rosser⁶

showed that the ratio of doses at depths 2 cm to 5 cm (D_2/D_5) could be correlated to measured energy spectra in the laboratory environment; however spectrometry of this nature is not generally available in the clinical environment or in all calibration laboratories. Her measurements were also limited to a single experimental setup geometrically; this setup in itself would be extremely difficult to reproduce in the clinical environment. The measurement of D_2/D_5 in the clinical environment on the other hand, may be practical, and this underlies the major motivation for this work.

The HVL is measured under narrow beam, i.e., “good geometry” conditions, where a large distance between the absorber and the detector is maintained. If the beam has a low filtration or contains an appreciable amount of low-energy components in the spectrum, the slope of the attenuation curve decreases more with increasing absorber thickness. Thus different HVL beams can be obtained from such a beam by introducing different added filtration. In general, HVL increases with increasing filter thickness as the beam become increasingly harder i.e., contains a greater proportion of higher-energy photons. Beyond a certain thickness however, additional filtration may result in softening of the beam from a relative increase in Compton scattering. Since an increase in filtration results in a reduction in the available exposure rate, added filtration is carefully chosen to obtain a suitable HVL at an acceptable beam output. Increasing voltage across the tube also improves the beam penetration. Because x-ray beams have a spectral distribution of energies, which depend on voltage as well as inherent and added filtration, it is not possible to characterize beam quality in terms of the degree of beam hardening only⁵.

An alternate rule of thumb for energy specification is sometimes used where the average Bremsstrahlung x-ray energy is assumed to be approximately one-third of the maximum energy or maximum kVp. Of course, the one-third rule is a rough approximation since it ignores any contribution from the characteristic radiation, which can be significant at these energies⁵.

1.2.1 Survey of the kilo-voltage radiotherapy centers in the UK

A survey of low and medium-energy radiotherapy units in clinical and laboratory environments was conducted in the UK to assess the variation of HVL with nominal generating potential⁶. Figures 1-1 and 1-2 emanating from this survey showed that there was little agreement between these beam quality specifiers for all energies. Since these were the HVLs obtained from different hospitals, the data also indirectly reflects the uncertainties in the measurement of the HVL or the determination of the exact generating potential. These figures also showed that the hospital qualities deviated largely from the national standards laboratory (NPL) qualities. Since orthovoltage units in most hospitals can also suffer from a lack of output constancy and the absence of internal dose detectors with feedback, further uncertainties in these results can be expected.

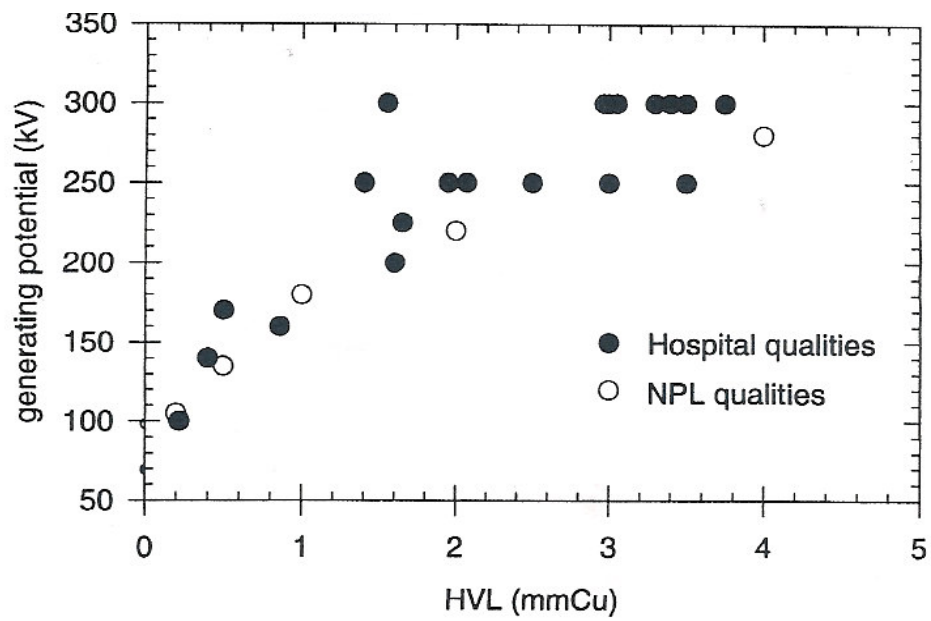
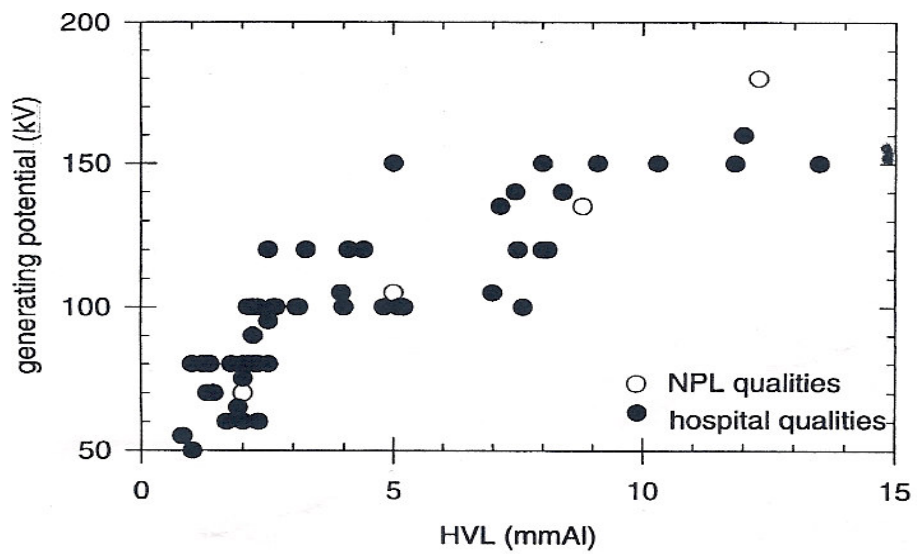


Figure 1-1. Variation in the half-value layer (HVL) with the generating potential for 26 UK radiotherapy centers at medium energies⁶.



1.3 NEED FOR THE STUDY

Low and medium energy kilo-voltage dosimetry codes of practice such as IPEMB Code of Practice, TRS 277³ and ICRU Report 23¹⁵ have ignored the need to measure the quality of the beam directly at the reference point of the absorbed dose measurement in water. Both the IPEMB¹⁰ and the ICRU¹⁵ recommend that for x-rays generated below 400 kV, the HVL in this energy range (low and medium) is the preferred beam quality index. However, HVL does not uniquely define the quality of a beam as x-rays having a particular HVL may be produced either by light filtration of high-voltage radiation or by heavy filtration of low-voltage radiation.⁵ Clinical and calibration laboratory beams often suffer from this discrepancy, as is the case in South Africa. IAEA TRS 277³, used for absolute dosimetry in radiation oncology, and BJR Supplement 25, used for relative dosimetry, have attempted to address this problem by tabulating their reference beam qualities using both parameters, i.e. the generating potential and HVL⁶. However, no advice is given on the method of handling dosimetry if the user's parameters differ from those in the documents. In these cases, the HVL alone is then normally taken as a beam quality specifier clinically.

1.4 RESEARCH OBJECTIVE

Specification of radiation beam quality arises from the fact that several parameters required for absorbed dose determination depend on the source energy. Thus the aim of this research is to compare and analyze two clinically measurable beam quality specifiers, the HVL and D_2/D_5 for kilovoltage modalities, and to determine whether a practical, alternative and/or better correlation exists. These would also be compared to the results published by Rosser⁶.

2. FACTORS AFFECTING THE QUALITY OF X-RAY BEAMS

2.1 THE QUALITY OF X-RAYS

Since radiation therapy relies on knowledge of the penetration of the beam into or through the patient, it is logical to describe beams in terms of their ability to penetrate some material of known composition. Johns and Cunningham⁷ recommend that beam quality is expressed in terms of the half value layer. The HVL is defined as the thickness of a given material of known composition required to reduce the beam intensity to half its original value. Over the range 120 kV to 400 kV, half value layers are usually given in mm of copper, while below 120 kV, aluminium is used.

The specification of the beam quality in terms of HVL is however a very basic specification, since it reveals very little concerning the number and energy of the photons present in the beam. Complete specification of the quality requires knowledge of the spectral distribution, i.e., the amount of energy (energy fluence) present in each energy interval. However, spectral distributions are difficult to measure on clinical units and a completely detailed specification may not be necessary, because the biological effects of x-rays are not very sensitive to the energy of the radiation. For this reason, the specification of beam quality in terms of HVL is usually considered sufficient⁵.

2.2 EFFECTS OF FILTERS ON AN X-RAY BEAM

When mono-energetic electrons bombard a thick target the spectral distribution of the unfiltered beam is linear, as shown in curve A of figure 2-1. This distribution would not in fact be suitable clinically since the low energy photons merely increase the dose to the superficial layers of the body relative to the dose at any given depth, and nor would they penetrate through a patient to reach an external imaging device. The unwanted low energy radiation may be removed from the beam by the use of appropriate filters⁷. From figure 2-1, curve B results when curve A is filtered by 1 mm aluminium.

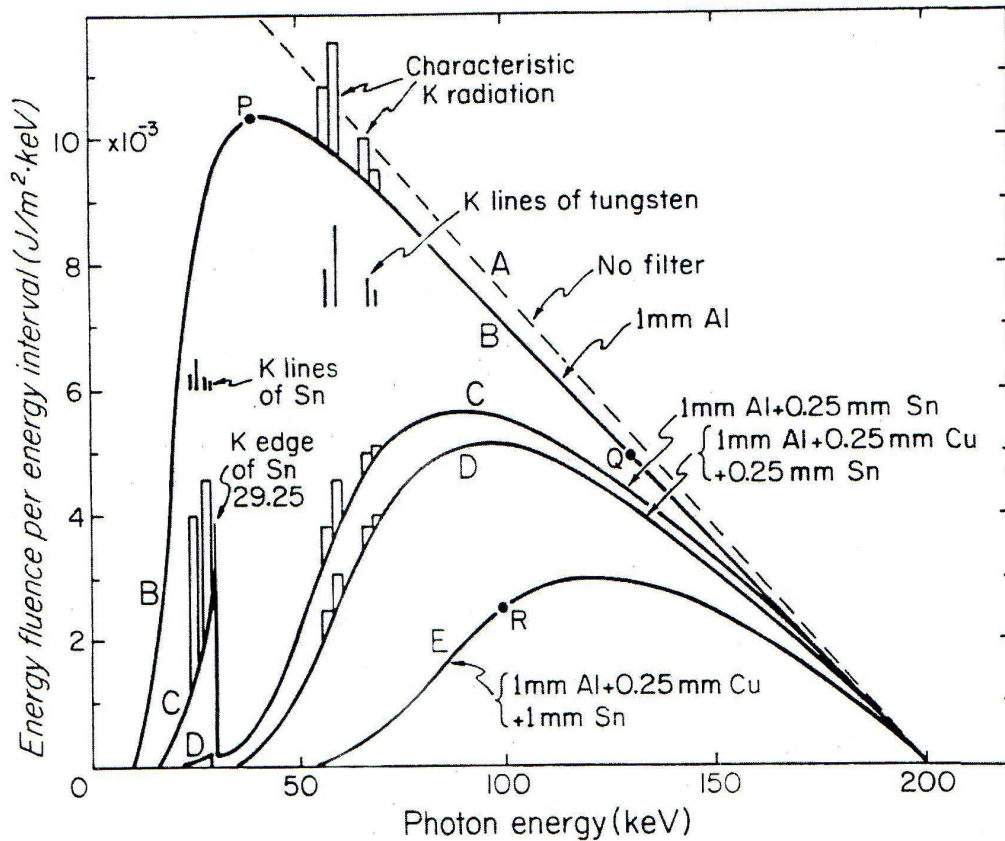


Figure 2-1. Graph showing how the spectral distribution of radiation generated by 200 keV electrons bombarding a thick tungsten target changes with filtration. Dashed line A, unfiltered beam. Curves B, C, D, and E are obtained from A by calculating the attenuation produced by the indicated layers of Al, Cu, and Sn⁷.

Curve C results when an additional 0.25 mm tin filters the beam of curve B. It can be seen that this practically reduces the energy fluence to zero in the region of 30 to 40 keV but allows a band of radiation to pass through the filter just below the K absorption edge of tin at 29.2 keV. Above 29.2 keV the tin absorbs x-rays strongly by the photoelectric process, but just below this energy the photons have insufficient energy to eject the K-shell electrons, so the photoelectric absorption is small. In addition, the photons that strongly interact with the tin by the photoelectric process above 29.2 keV will produce tin atoms with vacancies in the K shell and when these vacancies are filled, the characteristic radiation of tin at energies from 25 to 29 keV will be produced. This characteristic radiation will add to curve C as indicated by the absorption edges. Radiation below 29.2 keV may be filtered out by placing a thin layer of copper between the tin filter and the patient as shown by curve D. The copper absorbs strongly in the region below 29.2 keV and so removes most of the low energy from curve C. In addition, the copper strongly absorbs the characteristic radiation of tin. It is usual to place a thin layer of aluminium next to the copper to absorb the characteristic radiation from the copper. Composite filters of this kind are called Thoraeus filters. It is important that these filters are arranged in the correct order with the highest atomic number material nearest to the tube; otherwise, the characteristic radiation would not be stopped.⁵ A more penetrating beam (E) can be obtained by further filtration of D⁷.

2.3 THE MEASUREMENT OF HALF VALUE LAYER

The half value layer of an x-ray beam can be obtained by measuring the exposure rate of an x-ray machine for a series of different attenuators placed in the beam. The arrangement is indicated in figure 2-2 below.

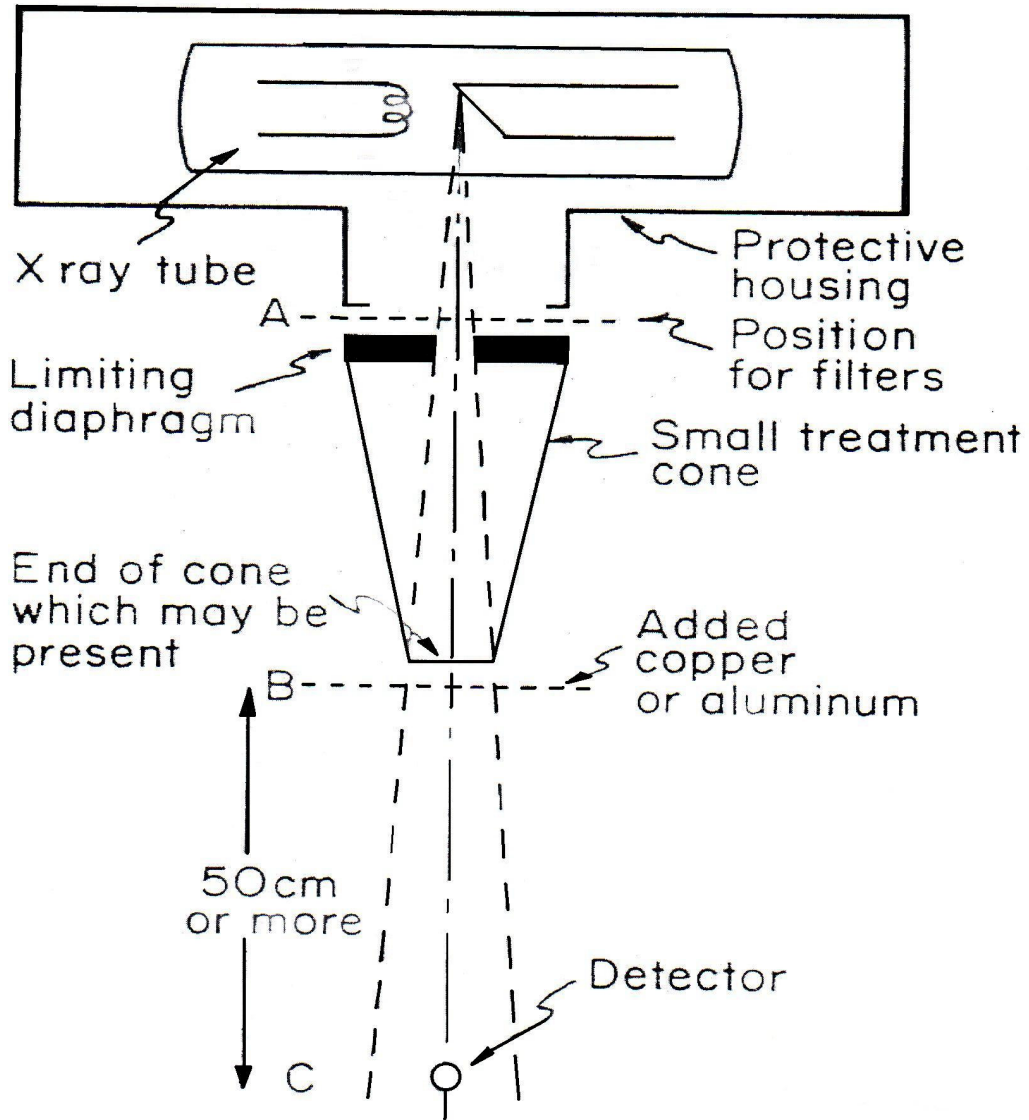


Figure 2-2. An ideal arrangement for accurate measurement of the half-value layer (HVL)⁷.

The sensitive volume of the dosimeter should be positioned with a clamp at point C on the central axis of the beam. The detector should be at least 50 cm from the end of the treatment cone or the beam-defining system of the unit so that radiation scattered by the attenuators is avoided. In addition, the x-ray beam should be directed in space such that the detector is at least 50 cm from any other scattering objects such as the floor or the walls. The beam from the machine should be limited to about 5 cm x 5 cm at the detector. Care should be taken to ensure that the detector is in the centre of the field. When the x-ray machine is provided with a light localizer and continuously adjustable diaphragms, centering of the detector is easily carried out. The x-ray unit is generally provided with a holder at A into which different filters may be positioned. A clamp should be arranged to hold the additional attenuators of aluminium or copper in place. A series of such attenuators of about 5 cm x 5 cm in area should be used. Care should be taken to ensure that the aluminium or copper attenuators are of uniform thickness and do not contain impurities as do many alloys. A monitor chamber can be used to correct for variations of air-kerma rate, especially when the air-kerma rate is significantly lowered by the addition of filtration in the beam during the HVL measurement. In that case, it must be placed such that it does not perturb the narrow beam by adding to the scatter component, and its response should not be affected by the thickness of the attenuating material⁸.

The exposure rate or air-kerma rate should be determined for a series of attenuators placed at B, while the kV and mA of the tube are held as constant as possible. Results of a typical experiment are shown in figure 2-3⁷. It is expected that an exponential attenuation curve should appear as a straight line when plotted on semi log paper. The curve is not linear when the beam of radiation from the x-ray tube is not monoenergetic. However, under heavy filtration, the softer components are almost completely removed and the radiation transmitted approaches monochromaticity in which case, the attenuation curve may approach a straight line⁷.

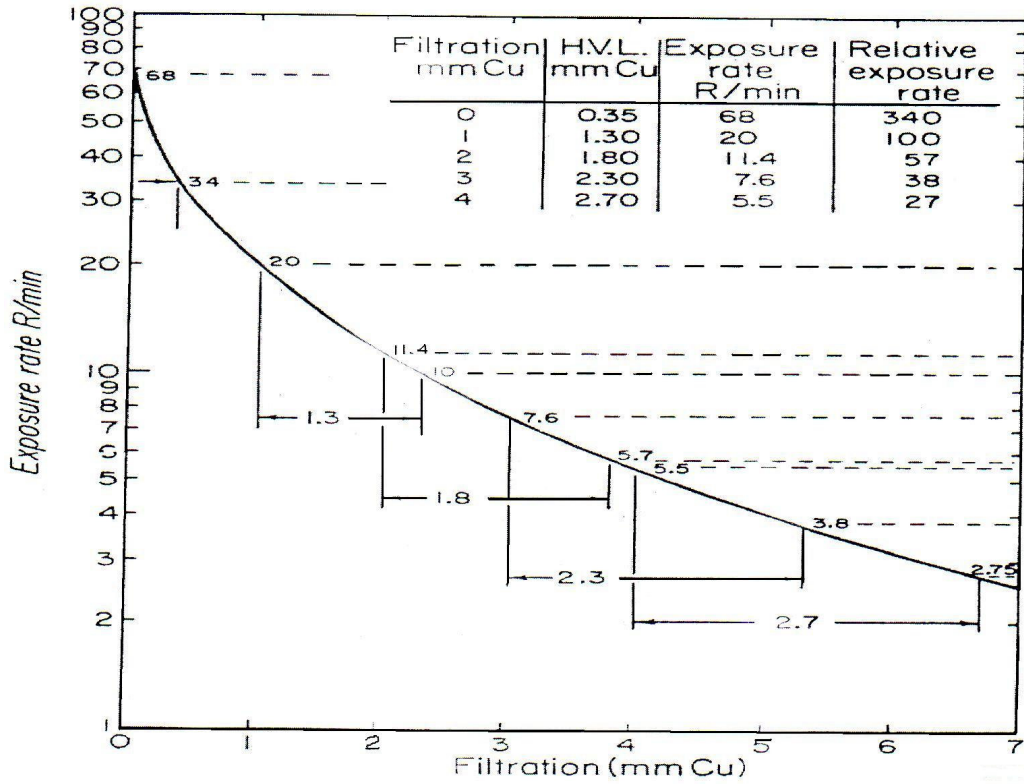


Figure 2-3. Experimentally determined attenuation curve for 200 kV radiation, showing how the HVL may be determined for a number of filtrations⁷.

After obtaining the data of figure 2-3 the user would then decide on the filter to be used in the routine operation of the machine and the appropriate filter or filters would be locked into place in the filter slot. The beam from the machine with the filter at A (figure 2-2) might now be slightly different from the beam with filter at B because of the influence of scattered radiation from the cone or material on the end of the cone.

2.4 EFFECT OF SCATTER ON HVL MEASUREMENTS

If scattered radiation is not avoided, very erroneous values for the HVL may be obtained as shown in figure 2-4, where HVL experiments were performed on a 250 kV unit using different diaphragm widths⁷. The HVL discrepancy arises from the effects of scattered radiation. With the attenuator at A, a negligible fraction of the scattered radiation reaches the detector, whereas if it were placed at B, because of its close proximity to the detector, a large fraction of the scattered radiation would reach P. These two conditions are referred to as attenuation experiments in “good geometry” and “bad geometry” respectively. Altering the field size, also illustrated in figure 2-4, may also change the HVL results. The correct HVL is considered to be the minimum value (2.0 mm Cu), obtained in the experiment in which most of the scattered radiation from the attenuator was avoided.

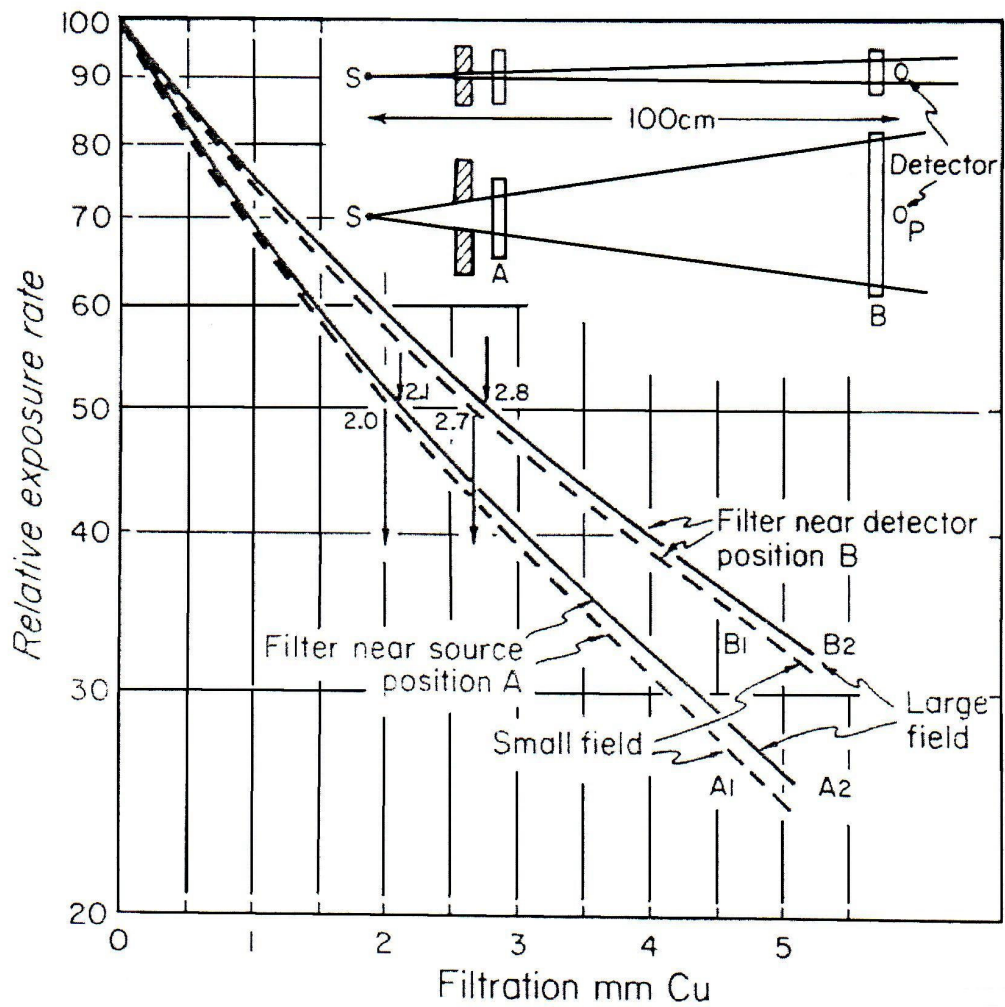


Figure 2-4. Diagrams to illustrate how different apparent half-value layers may be obtained for the same beam using different arrangements of field size and attenuator position during the measurements⁷.

2.5 EFFECTS OF DETECTOR ON HVL MEASUREMENT

The measurement of HVL requires the availability of an air-filled ionization chamber with a calibration factor that does not vary significantly at low to medium energies such that the estimated uncertainty is limited to less than or equal to 2%.⁸ If the measuring device does not exhibit such a flat response, an error will be introduced into the HVL measurement, since the spectrum and hence the response will be dependent on the amount of attenuator added during the HVL determination. An extreme example of this situation is illustrated in figure 2-5, where an attenuation experiment was performed on a 130 kV x-ray beam used in CT scanning⁷. Two sets of measurements were carried out. One set, using a calibrated air wall detector, with low energy photons, gave an HVL of 5.7 mm Al. The second set, obtained using a high-pressure xenon chamber as the detector, gave an incorrect HVL of 8.6 mm Al. The air wall detector gave a reading proportional to the energy absorbed in air while the xenon detector gave a reading essentially proportional to the energy fluence of the beam. The difference between the two curves is a striking illustration of the effects of “detector response” on the measured HVL.

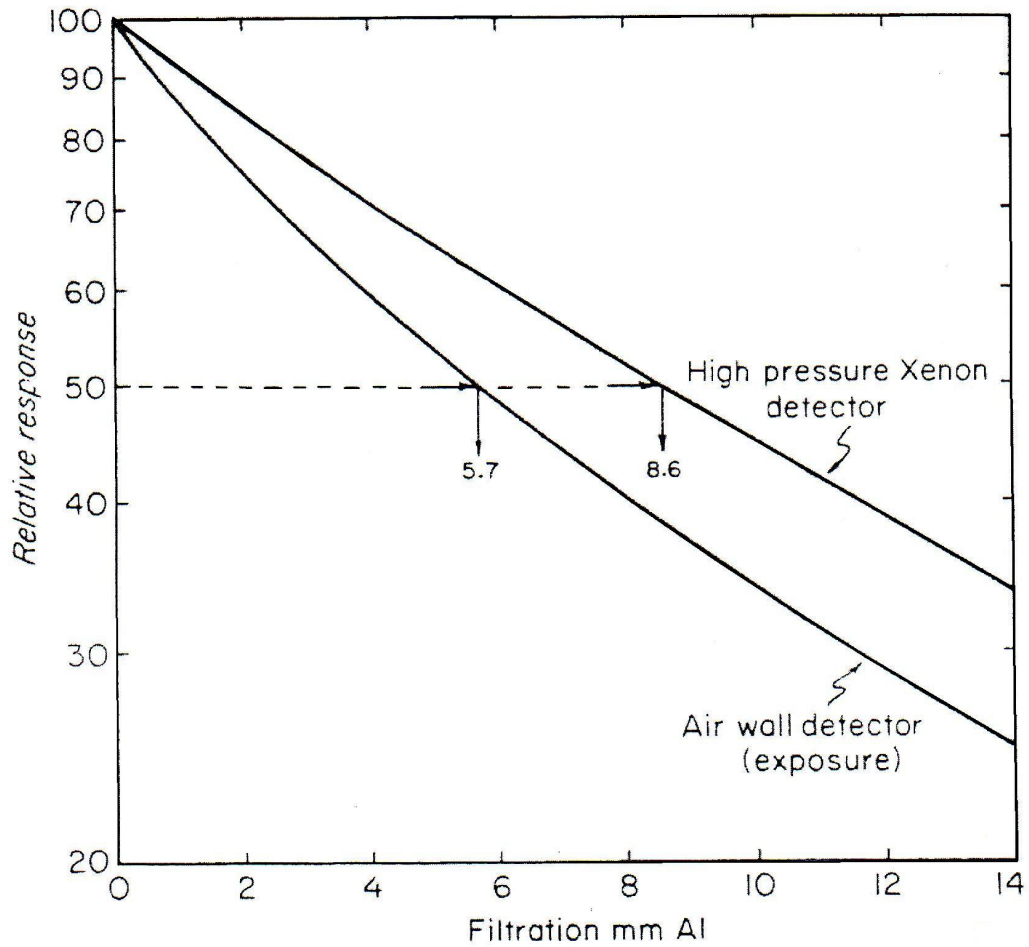


Figure 2-5. Graph showing how the measured attenuation of a beam from a 130 kV x-ray machine depends upon the type of detector used in the experiment ⁷.

2.6 HVL AND FILTERS FOR THERAPY

When 200 to 400 kV machines were introduced into radiotherapy, the precise determination of the HVL was essential because it was effectively used to determine the depth dose distribution. Cobalt 60 and Cesium-137 emit known spectra so energy specification is not required. Although the specification of HVL as 1.1 cm Pb for cobalt-60 is true, it is not a necessary statement; as it is possible to specify the average energy as 1.25 MeV. Linear accelerators of 4 to 20 MeV and betatrons of 20 to 30 MeV produce a continuous distribution of bremsstrahlung radiation from about 1 MeV to their peak energy. For these energies there is essentially no good filter material. In these cases, beam quality specification is based on relative dosimetry in water.

3. CODES OF PRACTICE IN KILOVOLTAGE THERAPY

3.1 HISTORICAL REVIEW

Kilovoltage x-ray beams continue to be used in radiation therapy and radiobiology. According to a survey conducted in 1995 by American Association of Physicists in Medicine (AAPM)⁸, there has been a renewed interest in radiotherapy treatment with superficial and orthovoltage x rays, with more kilovoltage machines being ordered and installed in North America during the last decade. In 1973 the ICRU Report No. 23¹⁵ recommended “the in-air method” for dosimetry of low-energy photons (tube potential: 40–150 kV) with the backscatter factors taken from the 1961 British Journal of Radiology BJR Supplement 10 and “the in phantom method” for dosimetry of medium-energy x rays (tube potential: 150–300 kV). In 1981, the National Council on Radiation Protection and Measurements formulated the dose to a phantom material from a point in air (with a minimum phantom) for tube potentials 10 kV up to 300 kV⁸. In 1987, the IAEA code of practice also recommended two different formalisms for low and medium energy photons although the beam quality ranges were defined differently (low energy: tube potential 10–100 kV, medium energy: tube potential 100–300 kV). The recommended backscatter factors were derived from Monte Carlo calculations. In 1996, the code of practice primarily intended for dosimetry in kilovoltage for radiotherapy from the IPEMB¹⁰ was published. The basis of this code of practice was the determination of the absorbed dose based on an air kerma measurement. The AAPM also recommended dosimetry procedures for kilovoltage x-ray beam dosimetry for radiotherapy and radiobiology applications⁸.

3.2 EQUIPMENT

3.2.1 Dosimeters

Air-filled ionization chambers are used for reference dosimetry in kilovoltage x-ray beams^{3, 8, 11, 12}. A cylindrical chamber is robust and simple to use for measurements in a water phantom. The chamber volume should be between about 0.1 cm³ to 1.0 cm³, a compromise between the need for sufficient sensitivity and the ability to measure at a point^{3, 12}. The effective point of measurement in kilovoltage x-rays for cylindrical

chambers is the centre of the sensitive air cavity of the chamber. Measurements for medium-energy x-rays are performed with the effective point of measurement of the chamber placed either at 2 cm (5 cm in some codes of practice) depth in water (in cases where the dose at greater depths is of primary interest) or free in air (in cases where the surface dose is of primary interest)^{8, 13}. Cylindrical chambers that have a calibration factor varying with the beam quality by less than 3% within the energy range of interest should be used for reference dosimetry.

3.2.2 Electrometers

A charge or current-measuring device, normally termed an electrometer, measures an ionization chamber's response. This device is capable of reading currents of the order of 0.01 nA, with an accumulated charge of 50–100 nC. If calibrated separately from the ionization chamber, the electrometer correction factor is applied as part of the corrected ion chamber reading, M . This correction factor is generally close to 1.000 but occasionally can differ from unity by as much as 5%⁸. If the combination of electrometer and ionization chamber is calibrated as one system, no separate electrometer correction is needed (i.e., $P_{elec} = 1$)⁸. It should be possible (at least if the chamber is used in pulsed beams) to vary the voltage applied to the chamber in order to determine the ion collection efficiency and to reverse the polarity, so that the polarity effect of the ionization chamber may be determined.^{3, 12}

3.2.3 Phantoms

When using an in-air method, measurements are performed free in air, and no phantom is involved^{8, 13}. When using an in-phantom method, water is the preferred phantom material and the phantom size should be at least 30 x 30 x 30 cm³ or larger⁸. For convenience, plastic phantoms may be used for in-phantom routine quality assurance however, they should not be used for reference dosimetry as chamber correction factors and the conversion factors to derive dose at a depth in water are not well known³. In addition, the water equivalence of some commercial plastics for kilovoltage energies remains an area of active investigation⁸.

3.3 RADIATION QUALITY SPECIFICATION AND DETERMINATION

The radiation quality of an x-ray beam is normally characterised by tube potential, total filtration and first HVL⁸. The dependence of calibration factors as well as correction, conversion and backscatter factors on the radiation quality is expressed as a function of HVL in aluminium or copper. A measurement of HVL may be affected by the details of the experimental set-up, the procedures and the energy dependence of the dosimeters used. Detailed information about the target and the target angle, the materials in the beam and their thicknesses are required for accurate HVL calculations. It is generally considered to be insufficient to use only tube potential or HVL to specify a beam. Commonly used clinical beams have been reported to have a wide range of HVL values corresponding to the same tube potential⁶. Chamber-related factors, such as the calibration factor (N_K) and the overall correction factor ($P_{Q, \text{cham}}$), as well as the detector-independent mass energy-absorption coefficients for water to air and the backscatter factors, can vary for x-ray beams of the same tube potential but different HVL values, and vice versa. Although dosimetry data are increasingly derived as a function of both tube potential and HVL, the use of both tube potential and the HVL value may not completely resolve the specification problem for all the quantities involved⁸. This is because it is often impossible to match both the HVL and the kV used clinically, with the secondary standards dosimetry laboratory (SSDL) combination¹³. Moreover, in the context of a protocol, the addition of a dose calculation quantity in terms of which the data have to be presented increases complexity and the probability of clinical errors. It should however be stressed that the use of HVL as a quality index, poses a lot of uncertainties, which should not under any circumstances be overlooked.

3.4 A SUMMARY OF KILOVOLTAGE CODES OF PRACTICE OVER THE LAST FEW DECADES

The table below is a summary of the ICRU Report 23¹⁵, the IAEA TRS 277³, IPEMB Code of Practice¹⁰ and the AAPM TG-61⁸ Codes of Practice for kilovoltage dosimetry. These reflect the developments of kilovoltage dosimetry.

Table 3-1 A summary of the dosimetry of kilovoltage Codes of Practice.

Publisher	Beam quality specification	Dose formalism	
		Low energy	Medium energy
ICRU 1973	HVL	$D = R.k_1.k_2.N.F.\left(\frac{s+x}{s}\right)^2.B$	$D = R \times k_1 \times k_2 \times N \times F$
IAEA, 1987	HVL	$D_w = M_u N_K B k_u \left(\frac{\bar{\mu}_{en}}{\rho}\right)_{w,air}$	$D = M_u N_K k_u \left(\frac{\bar{\mu}_{en}}{\rho}\right)_{w,air} P_u$
IPEMB, 1996	HVL	$D_{w,z=0} = MN_k B_w [(\mu_{en}/\rho)_{w,air}]_{air}$	$D_{w,z=2} = MN_k k_{ch} [(\mu_{en}/\rho)_{w,a}]_{z=2,\phi}$
AAPM TG 61, 2001	HVL only or HVL + kV (generating potential)	$D_{w,z=0} = MN_K B_w P_{stem,air} \left[\left(\frac{\bar{\mu}_{en}}{\rho}\right)_{air}^w \right]$	$D_{w,z=2} = MN_K P_{Q,cham} P_{sheat} \left[\left(\frac{\bar{\mu}_{en}}{\rho}\right)_{air}^w \right]$

Where:

- $D_{w,z}$ is the absorbed dose at depth d in the undisturbed water phantom with the chamber removed;
- R is the instrument reading;
- k_1 is a factor to correct for any difference in temperature and pressure at the time of measurement from those prevailing when the instrument was calibrated;
- k_2 is a factor to correct for differences, such as quality, between the radiation field used for calibration and that being used;
- N or N_k is the calibration factor, determined by the standardizing laboratory at a stated quality of radiation, and under stated conditions of temperature and pressure.
- F is the historical composite coefficient relating the exposure in roentgens to the absorbed dose in water expressed in rad,
- s is the source to surface distance used in treatments;
- x is the distance between the locations of the surface and of the chamber centre,
- B or B_w is the backscatter factor appropriate to the field size and radiation quality,

- k_u and p_u are factors that account for variations in spectral distribution of X-rays used for the ionization chamber calibration free in air and that used in water, and allow for non-water equivalence of the chamber when in the user's beam, respectively,
- k_{ch} is a factor which accounts for the change in the response of the ionization chamber between calibration in air and measurement in a water phantom.
- $[(\mu_{en}/\rho)_{w,a}]_{z,\phi}$ is the mass energy absorption coefficient ratio of water to air, averaged over the photon spectrum at z depth in water
- $P_{Q, cham}$: overall correction factor to account for the effects due to the change in beam quality between calibration and measurement and to the perturbation of the photon fluence at the point of measurement by the chamber, and the chamber stem, which is dimensionless. and
- M is the instrument reading in coulomb obtained with a chamber after correction to standard pressure and temperature,

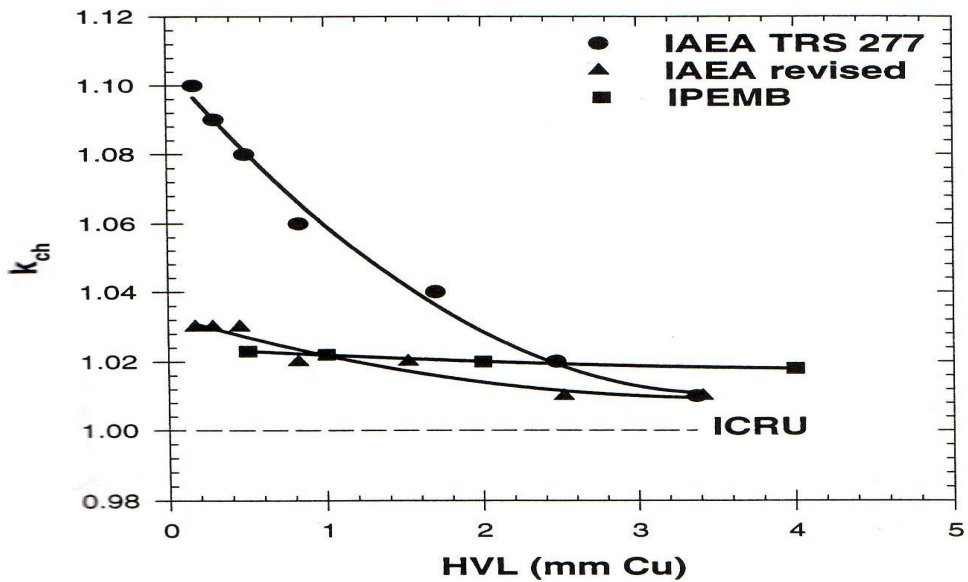
Over the years there has been a great deal of improvement in the dosimetry of high-energy photons and electron beams, but within this period there has been little or no change in the dosimetry of the kilovoltage energy range.¹⁴⁻¹⁷ Prior to the publication of the IAEA code of practice, TRS 277³, the main dosimetric reference was the ICRU Report 23¹⁵, in which exposure based calibration methods were used. For low-energies, the dose was determined indirectly from measurements taken in air as close as possible to the applicator end face, with the inverse square law being applied to take the reading back to the surface of the applicator¹⁵. For medium-energies, the reference depth of measurement was 5 cm in water.¹⁵⁻¹⁷ The beam quality was specified from the measurement of HVL.

The publication of the IAEA³ Code of Practice marked a new era in kV x-ray dosimetry. The roentgen-based F-factors were replaced by a formalism based on air-kerma and various correction factors were made more explicit. This brought about the introduction of new Monte Carlo (MC) based backscatters factor (B), which differed markedly from the standard values formally published in BJR supplement 17, and included chamber perturbation factors for medium-energies, which differed by as much as 10 % from unity^{2, 15}. The values of B in TRS 277 were confirmed by Grosswendt (1984, 1990) and Knight (1993, 1996) who employed MC simulations in a completely independent fashion and obtained virtually identical values.

The ionization chamber correction factors, denoted by p_u in TRS 277, were found to be incorrect (Hohlfeld 1993), and were revised in 1997.¹⁴ Figure 3.1 shows the changes made to chamber correction factors across the medium energy range.

In the IPEMB¹⁰ Code of Practice, K_{air} is converted into water kerma, K_{water} (through the mass energy absorption coefficient ratio, water to air), but free-in-air conditions are still used, i.e. for the primary spectrum (see appendix A). The backscatter factor (which is a ratio of water kermas) converts K_{air} , free in air, into water kerma at the surface of a water phantom. This procedure differs from TRS 277, where the B is a ratio of air kermas, and the mass-energy absorption coefficient ratio is field size dependent. The two methods are formally equivalent. The IPEMB code of practice recommends 2 cm as the reference depth for dose determination because of its relevance in clinic and because of rapid reduction of dose with depth in the kV region. HVL is still used as the beam quality specifier in the IPEMB Code of Practice. The addendum to the protocol suggests a method for determination of absorbed dose in air, at all kilovoltage energies.¹³

AAPM TG-61 is an air-kerma-based protocol using an in-air calibrated ionization chamber. This protocol allows for the use of the in-air method throughout the entire 40–300 kV energy range. The most important reason for the division of low- to medium energy is to specify a lower limit to the medium energy range, below which the in-phantom method is not used. This code of practice acknowledges that it is insufficient to use only tube potential or HVL to specify beam quality although the HVL solely or in combination with the tube potential, is often used to characterize beams. The depth of 2 cm in water is adopted for medium energies.



COMPARISON OF THE VALUE OF K_{ch} GIVEN IN MODERN CODES OF PRACTICE

Figure 3-1. Comparison of the value of k_h recommended by the IPEMB, with the original IAEA³ and the revised IAEA (1993) values across the medium energy range¹⁴.

4. METHODS AND MATERIALS

4.1 EQUIPMENT

Four x-ray units were used: two Philips RT 250 units operated between 100 kV and 250 kV, a D3300 Gulmay Medical unit and a Pantak HF 420. The specifications for the two units for Philips RT 250 units were poorly known.

The D3300 Orthovoltage system generated therapeutic radiation beams in the range 40 kV to 300 kV over a wide range of tube currents and HVLs, with 3 mm Be inherent filtration and a target material of Tungsten at a target angle of 30° . X-rays are emitted from an MXR-321 oil cooled, bi-polar, ceramic x-ray tube, manufactured by Comet of Berne, Switzerland. The CP320 HT Generator, manufactured by Gulmay Ltd. powered the x-ray tube. A sub-tube assembly mounted to the x-ray tube carries the treatment filter, the system ionization chamber, the treatment applicator and the electrometer mounted in the tube stand carriage assembly, which is interfaced directly to the x-ray controller. The system includes pressure and temperature transducers for automatic ion chamber compensation.

The HF 420 unit is capable of operating with a variety of metal ceramic or ceramic x-ray tubes. It is however installed as a laboratory unit, which is very different from a clinical set-up. It has a selection of focal spots for both single and dual focus x-ray tubes with 7 mm Be filtration. It is capable of producing x-rays of energy up to 420 kV with the capability of tube voltage being continuously adjusted in 1 kV increments. The tube current is adjustable from 0 to 30 mA in 0.1 mA increments. Both the tube current and voltage accuracy reproducibility were rated to be within $\pm 1\%$ and $\pm 0.03\%$ respectively.

An optical bench with good geometry to avoid extraneous scattering from the surroundings, was used to measure HVL. A lead diaphragm thick enough to attenuate all primary beams to approximately 0.5%, was used. The diaphragm collimated the beam to a 5 cm diameter at the detector distance. A cylindrical ionization chamber, with an active volume of 0.6 cc and an electrometer manufactured by PTW-Freiburg were used. A water phantom with a volume of about 30 cm x 30 cm x 30 cm was used

for the measurements of absorbed dose to water. The phantom, which was locally designed, provided full scatter around the chamber.

4.2 HVL DETERMINATION

The determination of HVL involved the successive measurement of air-kerma at a point in the collimated narrow beam, as the thickness of the attenuating material in the beam was increased. A radiographic check of the alignment of the source, the diaphragm, and the detector was performed. Care was taken to avoid any scattering material around the detector position. As the study required a range of beam qualities (HVL), the energies were those as used clinically. This method was also in agreement with that used by Rosser⁶.

Figure 4-1 shows the experimental setup for the HVL measurement without a monitor chamber in place. Shown in the figure are the source (target), HVL attenuator, and the diaphragm for collimating the beam to about 2 cm focused onto the center of the ionization chamber. The ionization chamber used was sufficiently energy independent for a change in filter thickness not to introduce significant uncertainty in the measurements.

It is important to note that not all units housed an internal monitor chamber. A system was used therefore where the first measurement was repeated at the end of each series in order to ensure output constancy. An external monitor chamber was used on the Philips units, and the readings of the chamber were then normalized to the average of the un-attenuated readings from the monitor chamber. Figure 4-2 shows the experimental setup for HVL measurements with an external monitor chamber in place. The monitor chamber was located so that its response was independent of the thickness of attenuating material placed in the beam and such that it did not perturb the narrow-beam measurements by adding to the scatter component. This arrangement was used for those units, which did not have an internal monitor.

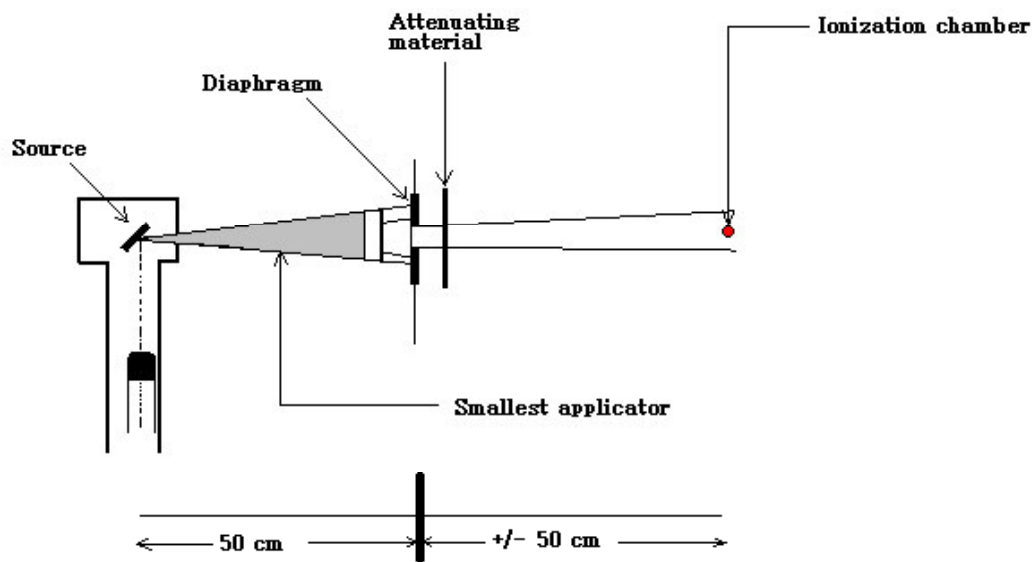


Figure 4-1. The experimental setup for an HVL measurement without a monitor chamber.

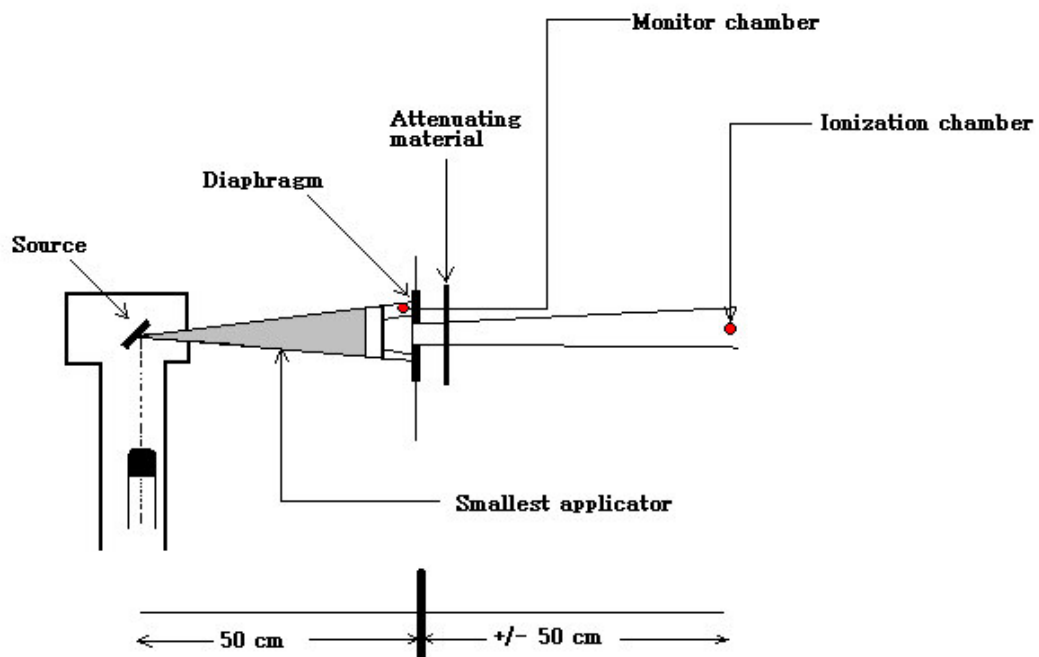


Figure 4-2. The experimental setup for an HVL measurement with a monitor chamber.

4.3 MEASUREMENT OF ABSORBED DOSE AT 2 cm AND 5 cm DEPTHS

A calibrated field chamber of 0.6 cc volume was used in a 30 cm x 30 cm x 30 cm water phantom to measure the absorbed dose to water at depths 2 cm and 5 cm in order to investigate the ratio of these doses as an alternative quality index. Measurements were made for a range of field sizes and focus to source distances (FSD), as given in Table 4-1. Verification of the inverse square law was performed as D_2/D_5 depends on it.

Table 4-1. Geometry used in the relative dose measurements.

<u>CONDITION</u>	<u>VALUE</u>
Field size at the surface of the phantom	range of field sizes
Depth in water	2 cm and 5 cm
Phantom size	30 cm x 30 cm x 30 cm
Source to surface distance	50 cm, and 1 m

5. RESULTS AND ANALYSIS

5.1 HVL RESULTS

5.1.1 Significance of a monitor chamber

In order to prevent the determination of misleading HVL results, an external monitor chamber was used⁸ for the units that did not have an internal monitor to compensate for instabilities in the x-ray machine output. Figure 5-1 demonstrates how an unmonitored output can give a different measurement of HVL at 100 kV on a Phillips RT 250 with an added filtration of 2.044 mm Al. Uncertainty in individual data points was about +/- 3%. These curves show how much an unstable x-ray unit or inadequate setup, can influence the outcome of fitting raw data to determine the HVL. This influences the lack of accuracy in dosimetry for these modalities.

5.2 RELATIONSHIP BETWEEN HVL AND GENERATING POTENTIAL

One of the most fundamental challenges in kilovoltage dosimetry is the lack of correlation in HVLs used clinically with generating potential when compared to national standards. As a result, a comparison between the beam qualities used by the SSDL in South Africa (CSIR) and those from international codes of practice, was made. Figures 5-2 and 5-3 compare how the CSIR beam qualities relate to other international standards at low and medium energies respectively. From these figures it is clear that there was general agreement between the SSDL's.

5.2.1 Comparison of clinical and laboratory beam qualities

Clinical beam qualities used in this work were obtained with the x-ray beam output monitored and corrected for. The beam qualities were plotted against generating potential and compared with the CSIR combinations. Figures 5-4 and 5-5 show how the measured clinical beam qualities differ from those of the SSDLs. The results confirm the discrepancy in matching generating potential and HVL for clinical and laboratory institutions.⁶

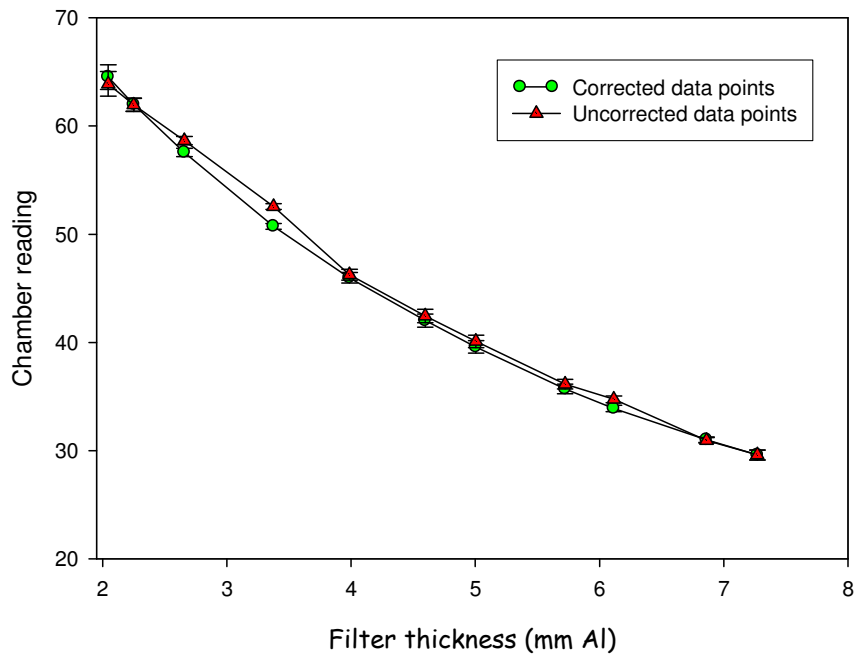


Figure 5-1. Two determinations of the HVL with the chamber readings corrected and uncorrected against the monitor chamber.

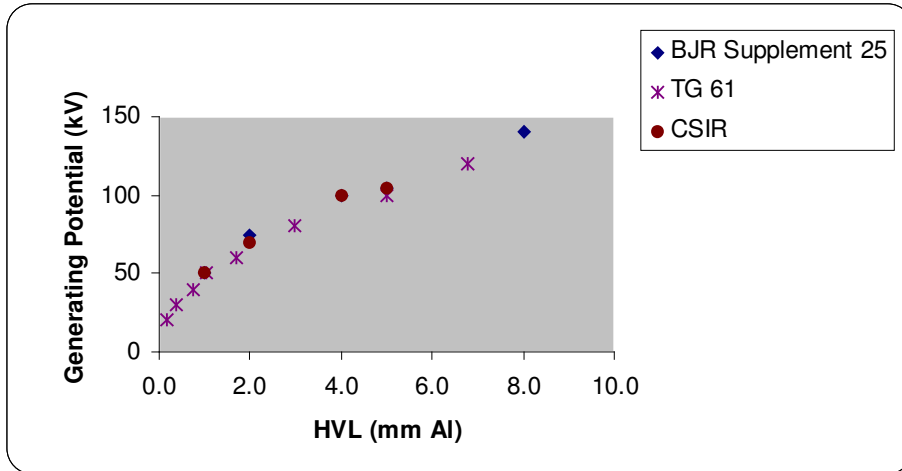


Figure 5-2. The relationship between HVL and generating potential for some SSDL and Codes of Practice at low energies.

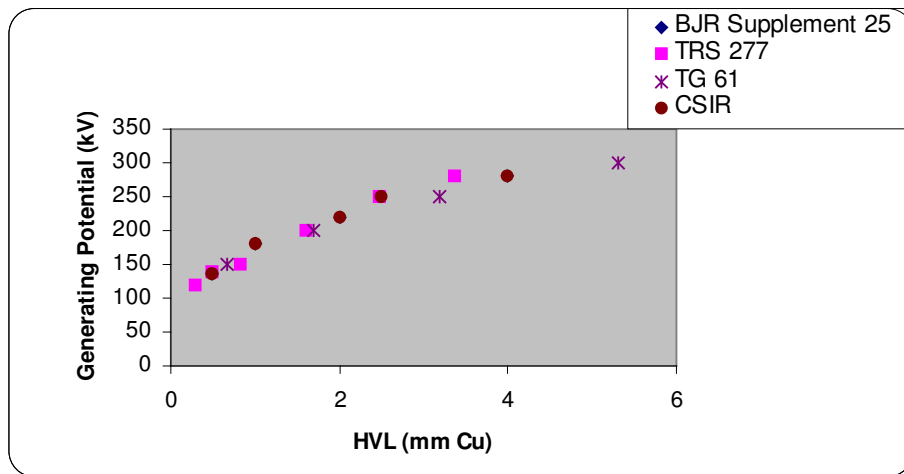


Figure 5-3. The relationship between HVL and generating potential for SSDL and Codes of Practice at medium energies.

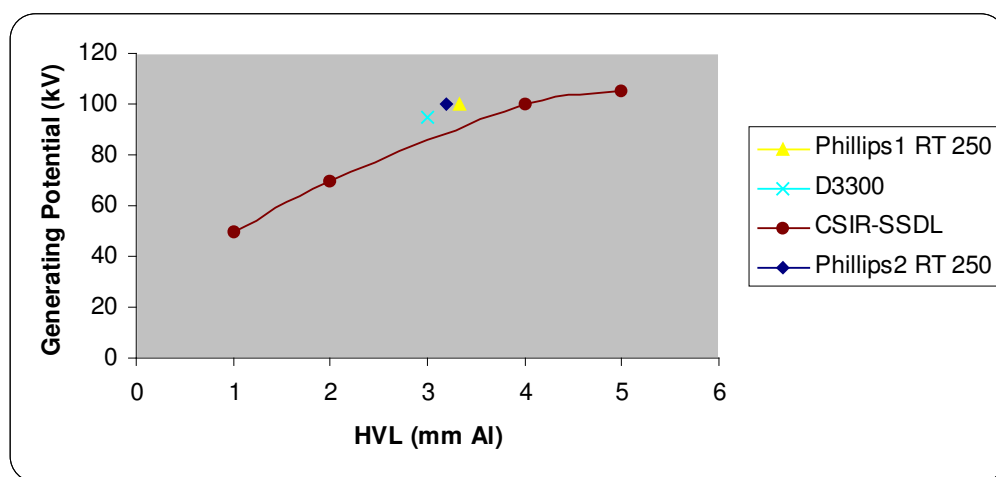


Figure 5-4. The variation of HVL with generating potential for hospital units and the South African SSDL at low energies.

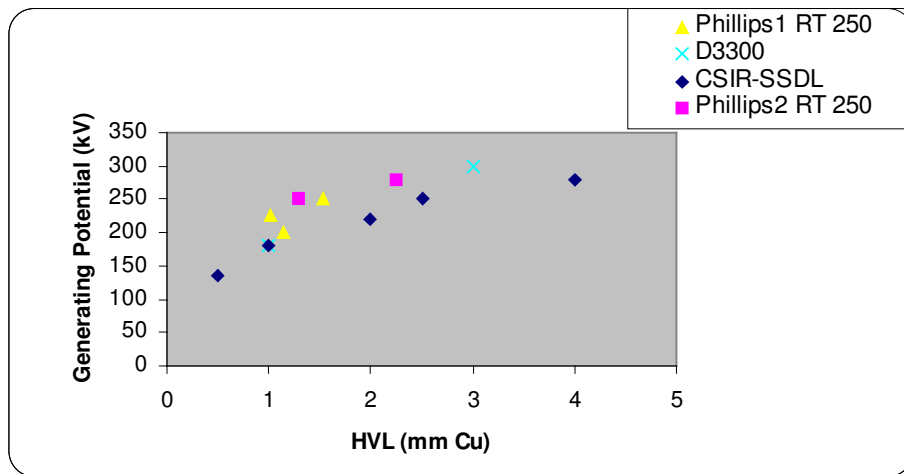


Figure 5-5. The variation of HVL with generating potential for the hospital units and the South African SSDL at medium energies.

5.3 COMPARISON OF HVL AND THE RATIO OF D_2/D_5 AS QUALITY INDEXES

An ideal beam quality index in radiotherapy using kilovoltage x-rays should be easy to measure and at the same time uniquely define the absorbed dose to water at the point of measurement⁶.

5.3.1 HVL as a beam quality index

HVL was measured for selected energies, and the added filtration was varied to obtain a number of beam qualities at the same energy. 100 kV and 250 kV from both the Philips RT 250 and the Pantak HF 420 were measured. The D3300 Gulmay medical unit was used at 300 kV. The energy dependent parameter of the absorbed dose to water, which is the ratio of the mass-energy absorption coefficient of water to air (MEAC), was studied as a function of HVL. The values of the MEAC used were from Knight based on the work published by Knight and Nahum²². Figure 5-6 shows the variation of MEAC with HVL at 100 kV whilst figure 5-7 shows the data at 250 kV and 300 kV.

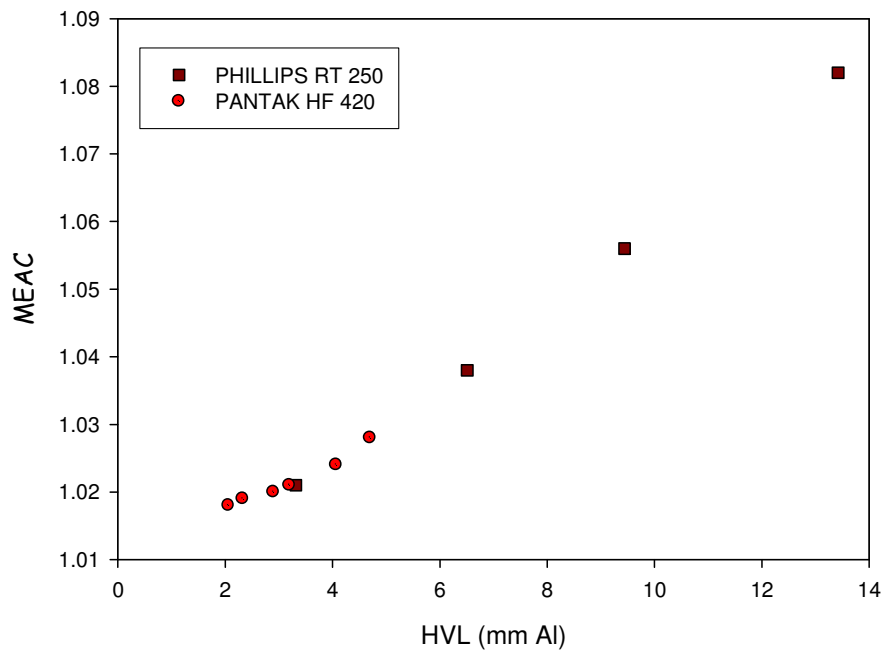


Figure 5-6. The relationship between the HVL at 100 kV and the MEAC.

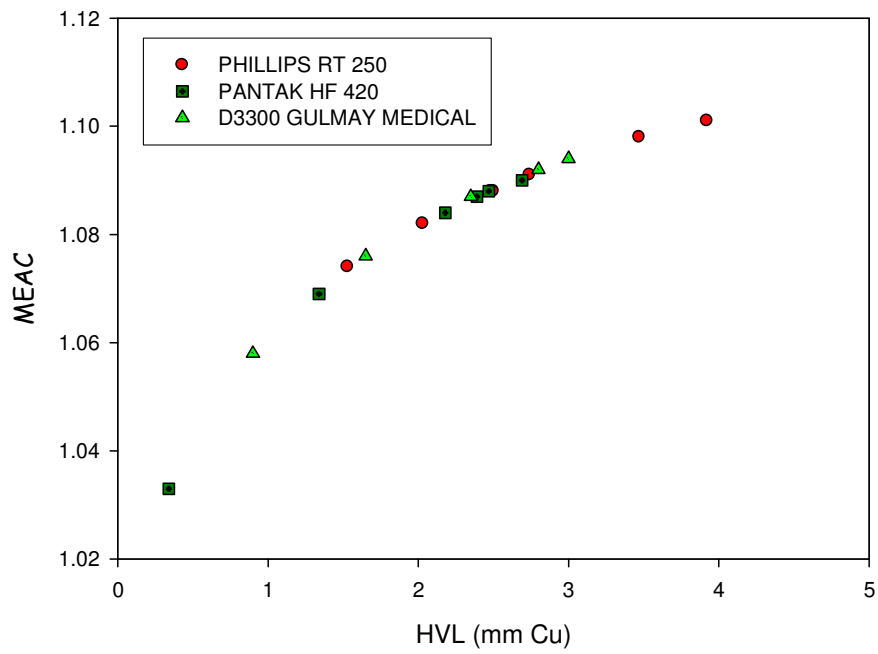


Figure 5-7. The relationship between the HVL generated at 250 kV and 300 kV and the MEAC.

5.3.2 D_2/D_5 as a beam quality index

The ratio doses at 2 cm and 5 cm depth in water (D_2/D_5) is theoretically given by equation 5.1 below⁶:

$$\frac{D_2}{D_5} = \frac{\left(MN_K k_{ch} \left[\left(\frac{\bar{\mu}_{en}}{\rho} \right)_{w/a} \right] \right)_{depth=2cm}}{\left(MN_K k_{ch} \left[\left(\frac{\bar{\mu}_{en}}{\rho} \right)_{w/a} \right] \right)_{depth=5cm}} \quad 5.1$$

There is currently no information on the variation of k_{ch} with depth but it is expected to be minimal¹³. It has been shown that there is a small correction for the variation of $\left(\left[\left(\frac{\mu_{en}}{\rho} \right)_{w,a} \right]_{z,\phi} \right)$ with depth^{6, 13}. For general dosimetry k_{depth} is assumed negligible as it varies between 0.999 and 1.004 at the beam quality range studied¹³. Equation 5.1 therefore can be approximated as:

$$\frac{D_2}{D_5} = \frac{M_2}{M_5} k_{depth} \approx \frac{M_2}{M_5} \quad 5.2$$

Measurements of D_2/D_5 were made with a 0.6 cc cylindrical chamber in a 30 cm x 30 cm x 30 cm water phantom. D_2/D_5 was measured on the Pantak HF 420 at an FSD of 100 cm with a field size of approximately 5.5 cm diameter. Measurements were also made on the D3300 Gulmay medical unit at the standard FSD of 50 cm with a range of field sizes i.e. 4 cm x 4 cm, 8 cm x 8 cm, 10 cm x 10 cm and 15 cm x 15 cm. Figures 5-8, 5-9 and 5-10 show how MEAC varies with D_2/D_5 at 100 kV, 250 kV and 300 kV respectively. Figure 5-11 is a plot of MEAC against D_2/D_5 at 300 kV for the series of different field sizes as well. It can be deduced from this figure that the shape of the graphs does not change with the field size even though D_2/D_5 decreases with increasing field size.

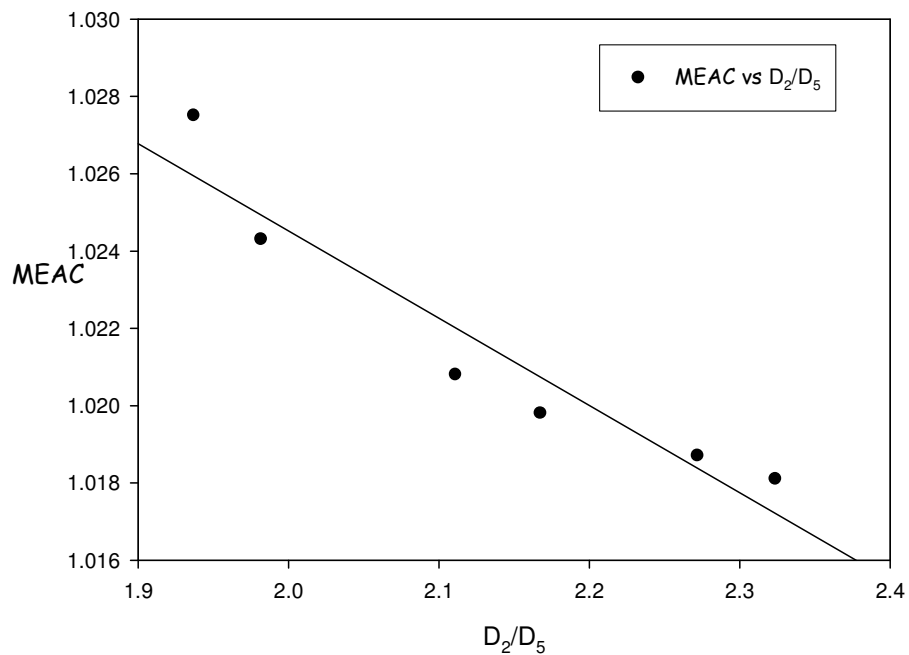


Figure 5-8. The variation in MEAC with D_2/D_5 at an FSD of 100 cm for different HVLs at 100 kV for the Pantak HF 420 unit. The solid line is the linear regression of the data points.

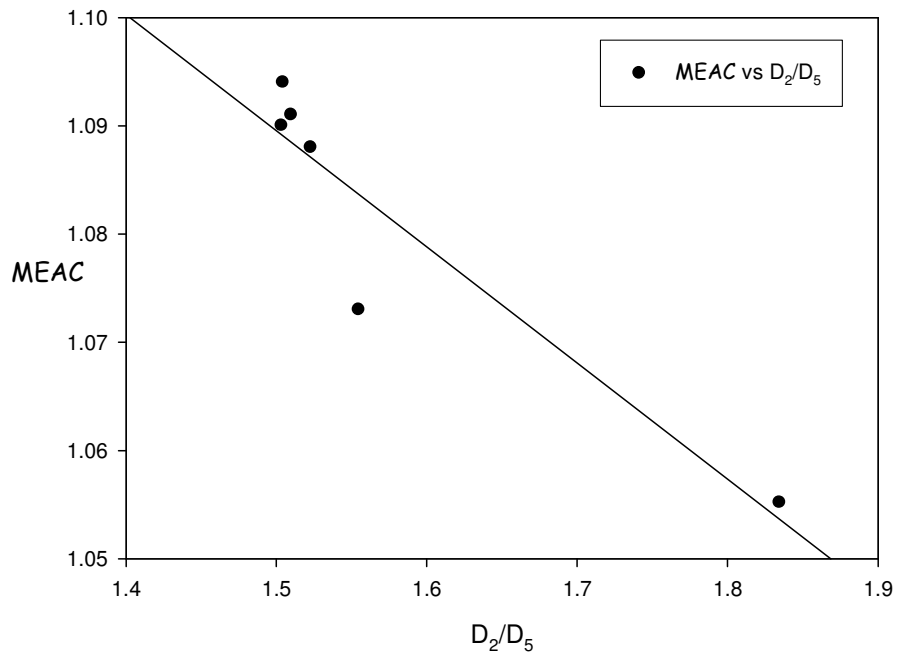


Figure 5-9. The variation in MEAC with D_2/D_5 at an FSD of 100 cm for different HVLs at 250 kV for the Pantak HF 420 unit. The solid line is the linear regression of the data points.

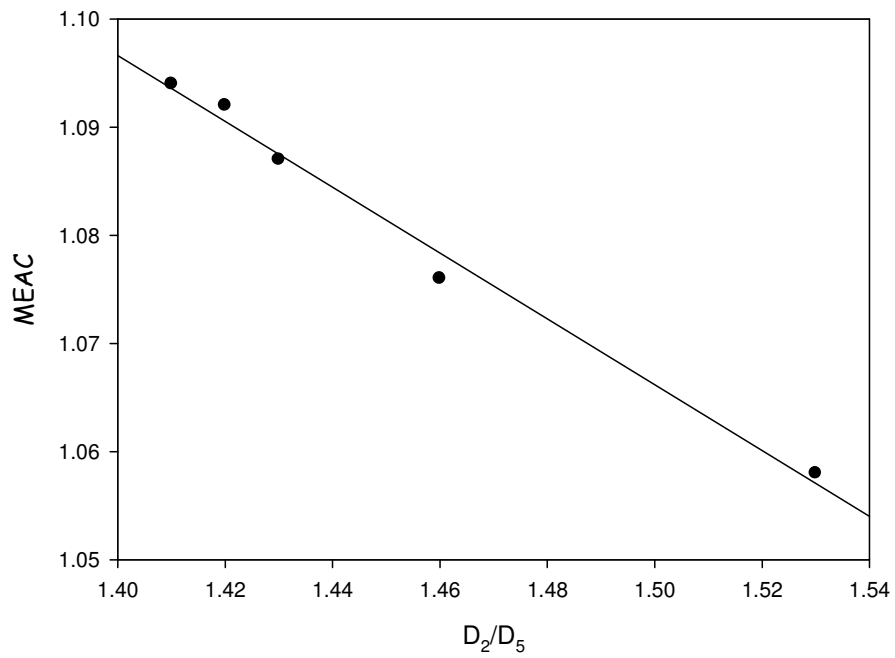


Figure 5-10. The variation in MEAC with D_2/D_5 at an FSD of 50 cm for different HVLs at 300 kV for the D3300 unit. The solid line is the linear regression of the data points. Measurements were taken at a field size of $10 \times 10 \text{ cm}^2$.

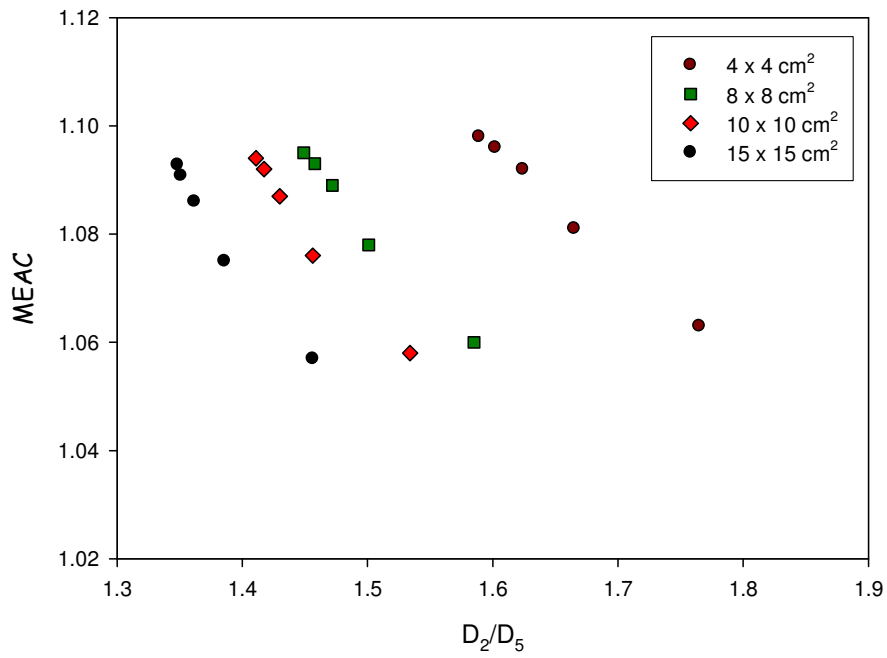


Figure 5-11. The variation in MEAC with D_2/D_5 as a function of different HVLs at 300 kV for the D3300 Gulmay Medical unit. Measurements were taken at the standard FSD of 50 cm and a range of field sizes are shown.

Figure 5-12 is a plot of D_2/D_5 as a function of HVL at low energies. Measurements were taken at 100 cm FSD with a field size of 5.5 cm diameter. Figure 5-13 is an equivalent plot for the medium-energies. Measurements were taken at the standard FSD of 50 cm in a 10 cm x 10 cm field. Each graph has been regressed and the relationship derived between D_2/D_5 (y) and HVL (x) is given in the figures. Compared to HVL, D_2/D_5 could be used as an alternative beam quality specifier in kilovoltage dosimetry clinically. The coefficient of correlation between D_2/D_5 and the HVL was calculated to be -0.99 and -0.94 for lower and medium energies respectively.

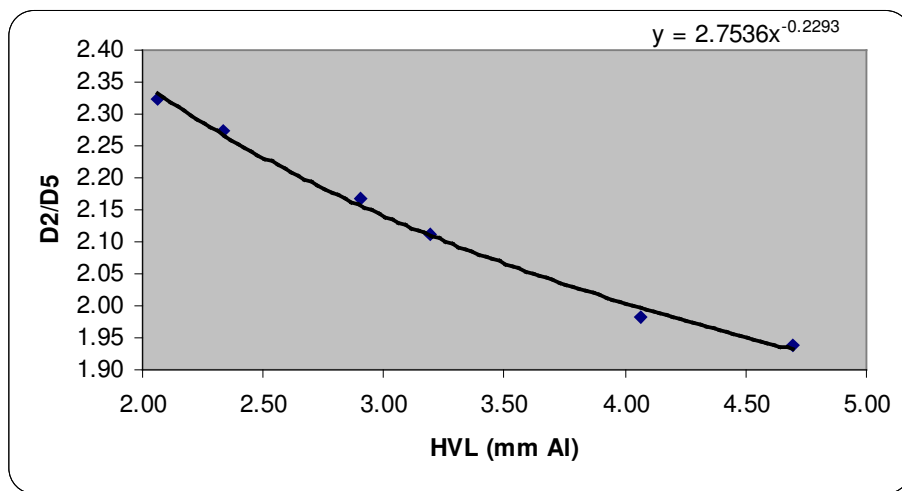


Figure 5-12. D_2/D_5 as a function of HVL at low energies. The solid line is the regression that best fits the data points to the resulting equation given on the graph.

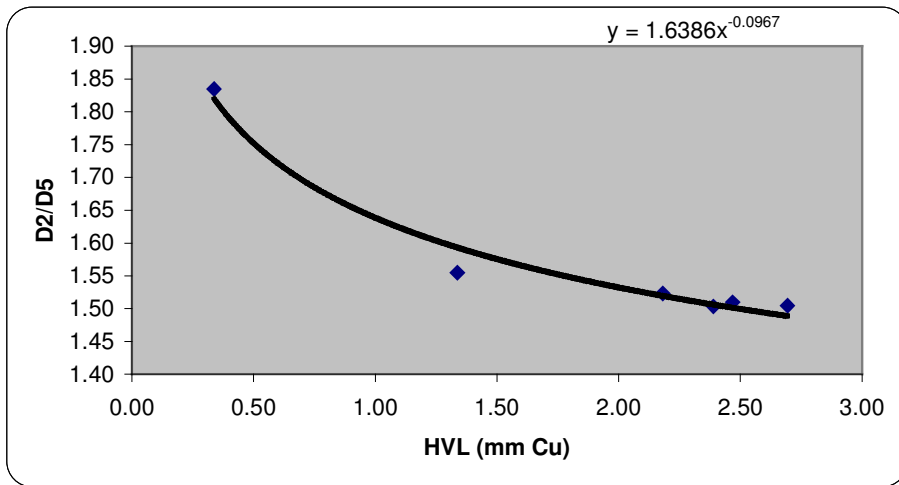


Figure 5-13. D_2/D_5 as a function of HVL at medium energies. The solid line is the regression that best fits the data points to the resulting equation given on the graph.

6. DISCUSSION

A beam quality index in clinical dosimetry should be easy to measure whilst at the same time uniquely define the absorbed dose to water at the point of measurement. Published PDD's are available as a function of beam quality (HVL) only and are widely implemented clinically. It is very critical that a suitable quality index is established.

Currently, most errors in the specification of kilovoltage beam quality can be attributed to the experimental setup of the measurement of HVL. Errors are also introduced from lack of stability in beam output on some units, especially those that are not equipped with internal dose monitors, as shown in this work. International Codes of practice advise users to introduce a monitor chamber to monitor the variation in machine output during such a suite of measurements. The effectiveness of using a monitor chamber in the determination of HVL has been shown to be significant in this work.

A comparison between data points of some international Codes of Practice and the CSIR was made in terms of the relationship between the generating potential and the HVLs for both low and medium energies. The results showed agreement between the qualities adopted by CSIR with those used by other international codes of practice. This was consistent with the results of Rosser⁶.

Comparison between the clinical and SSDL beam qualities showed however, that clinical beams are of arbitrary filtration. This introduces uncertainties as interpolations between HVLs are made for dosimetry purposes, i.e. errors in chamber calibration factors may result as hospital users interpolate between differently filtered beam series⁸. In such cases it is advised that interpolation should only be carried out between beams of the same filtration.⁸ The disadvantage of HVL as a beam quality specifier arises from the actual measurement as alignment of the apparatus and detector centering are difficult to achieve accurately. These measurements also require an optical bench; high purity filters and are time-consuming to perform. Setup

difficulties as a result, can introduce errors in the determination of absorbed dose to water.

A quality index can be used to define the absorbed dose to water if its energy dependence is known. MEAC, which was found to have significant variation with energy over this energy range (kilovoltage), has been used to study the energy dependence of the two quality indexes being investigated. The relationship between $([\mu_{en}/\rho]_{w,a}]_{z=2,\phi})$ and the HVL was consistent with the results shown by Rosser⁶ in terms of how HVL defines the ratio of mean mass energy absorption coefficient of water to air at 2 cm depth in water.

In this work, the low and medium energy graphs have been plotted on different axes, which is more clinically relevant. In Rosser's work⁶, the low and medium energies were highly and lightly filtered respectively to simulate extreme conditions, which may not be clinically relevant.

The ratio of dose at depths 2 cm and 5 cm was studied as an alternative beam quality index to HVL, and was found to be consistent with MEAC. D_2/D_5 for the SSDL unit at 100 kV and 250 kV were measured at an FSD of 100 cm with the field size collimated to approximately 5.5 cm diameter. This set-up of D_2/D_5 is however very different from that used in most clinical environments due to the fixed installation of the unit.

The same comparison was done on a clinical unit at 300 kV; and further measurements were taken at different field sizes (4 cm x 4 cm, 8 cm x 8 cm, 10 cm x 10 cm and 15 cm x 15 cm) at an FSD of 50 cm. This setup is more commonly used in the hospital environment as it is practical, clinically relevant, and easy to reproduce. Use of D_2/D_5 as a quality index at 10 cm x 10 cm is also more consistent with beam quality determination in megavoltage photon beams, e.g. the tissue phantom ratio at a depth 20 cm to that at depth 10 cm. A strong relationship was established between D_2/D_5 and the HVL.

This work was driven by the need to improve and simplify the beam quality specification in kilovoltage dosimetry. D_2/D_5 at the standard FSD and in a reference field size could be used as a unique beam quality specifier. Further work would have to be done to investigate other energies. Lower energies may require the use of shallower depths in order to improve accuracy and ensure a more clinically relevant setup.

7. CONCLUSIONS

- This project verified that the ratio of doses at depths 2 cm and 5 cm in water could be applied as a kilovoltage beam quality specifier in the clinical environment at low and medium energies.
- For beam quality specification in kilovoltage, a parameter based on a broad, central axis dose ratio in water at two specified depths is more realistic than a quasi-narrow beam quality measurement using non-tissue equivalent material (e.g. Al and Cu).
- D_2/D_5 is more consistent with beam quality specification in megavoltage photon beams where parameters such as the ratio of tissue phantom ratio at 20 cm to that at 10 cm depth in a water phantom are used.
- Measurement of D_2/D_5 in a typical field size of 10 cm x 10 cm and at the standard FSD is more practical and relevant to clinical institutions.
- With well-defined field sizes and FSD's, a relationship between HVL and D_2/D_5 was found.
- The use of D_2/D_5 as a tool to verify the beam quality index would simplify quality control in the clinical environment.

APPENDIX A

A. DOSIMETRIC PRINCIPLES

A.1 INTRODUCTION

Radiation measurements and investigations of radiation effects require various specifications of the radiation field at the point of interest. Radiation dosimetry deals with methods for the quantitative determination of energy deposited in a given medium by directly or indirectly ionizing radiations. A number of quantities and units have been defined for describing the radiation beam, and the most commonly used dosimetric quantities and their units are defined below. A simplified discussion of cavity theory, the theory that deals with calculating the response of a dosimeter in a medium, is also given.

A.2 PHOTON FLUENCE AND ENERGY FLUENCE

The following quantities are used to describe a monoenergetic ionizing radiation beam: particle fluence, energy fluence, particle fluence rate and energy fluence rate. These quantities are usually used to describe photon beams and may also be used in describing charged particle beams.

- The particle fluence Φ is the quotient dN by dA , where dN is the number of particles incident on a sphere of cross-sectional area dA :

$$\Phi = \frac{dN}{dA} \quad (\text{A.2.1})$$

The unit of particle fluence is m^{-2} . The use of a sphere of cross-sectional area dA expresses in the simplest manner the fact that one considers an area dA perpendicular to the direction of each particle and hence that particle fluence is independent of the incident angle of the radiation.

- Planar particle fluence is the number of particles crossing a plane per unit area and hence depends on the angle of incidence of the particle beam.
- The energy fluence Ψ is the quotient of dE by dA , where dE is the radiant energy incident on a sphere of cross-sectional area dA :

$$\Psi = \frac{dE}{dA} \quad (\text{A.2.2})$$

The unit of energy fluence is J/m^2 . Energy fluence can be calculated from particle fluence by using the following relation:

$$\Psi = \frac{dN}{dA} E = \Phi E \quad (\text{A.2.3})$$

where E is the energy of the particle and dN represents the number of particles with energy E . Almost all realistic photon or particle beams are polyenergetic, and the above defined concepts need to be applied to such beams. The concepts of particle fluence spectrum and energy fluence spectrum replace the particle fluence and energy fluence, respectively. They are defined respectively as:

$$\Phi_E(E) \equiv \frac{d\Phi}{dE}(E) \quad (\text{A.2.4})$$

and

$$\Psi_E(E) \equiv \frac{d\Psi}{dE}(E) = \frac{d\Phi}{dE}(E)E \quad (\text{A.2.5})$$

where $\Phi_E(E)$ and $\Psi_E(E)$ are shorthand notations for the particle fluence spectrum and the energy fluence spectrum differential in energy E , respectively. Figure 3-1 shows a photon fluence and an energy fluence spectrum generated by an orthovoltage X ray unit with a kVp value of 250 kV and an added filtration of 1 mm Al and 1.8 mm Cu (target material: W; inherent filtration: 2 mm Be). The two spikes superimposed on the continuous bremsstrahlung spectrum represent the K_α and the K_β characteristic X ray lines produced in the tungsten target. The particle fluence rate $\dot{\Phi}$ is the quotient of $d\Phi$ by dt , where $d\Phi$ is the increment of the fluence in time interval dt :

$$\dot{\Phi} = \frac{d\Phi}{dt} \quad (\text{A.2.6})$$

with units of $\text{m}^{-2}\cdot\text{s}^{-1}$.

The energy fluence rate (also referred to as intensity) is the quotient of $d\Psi$ by dt , where $d\Psi$ is the increment of the energy fluence in the time interval dt :

$$\dot{\Psi} = \frac{d\Psi}{dt} \quad (\text{A.2.7})$$

The unit of energy fluence rate is W/m^2 or $\text{J}\cdot\text{m}^{-2}\cdot\text{s}^{-1}$.

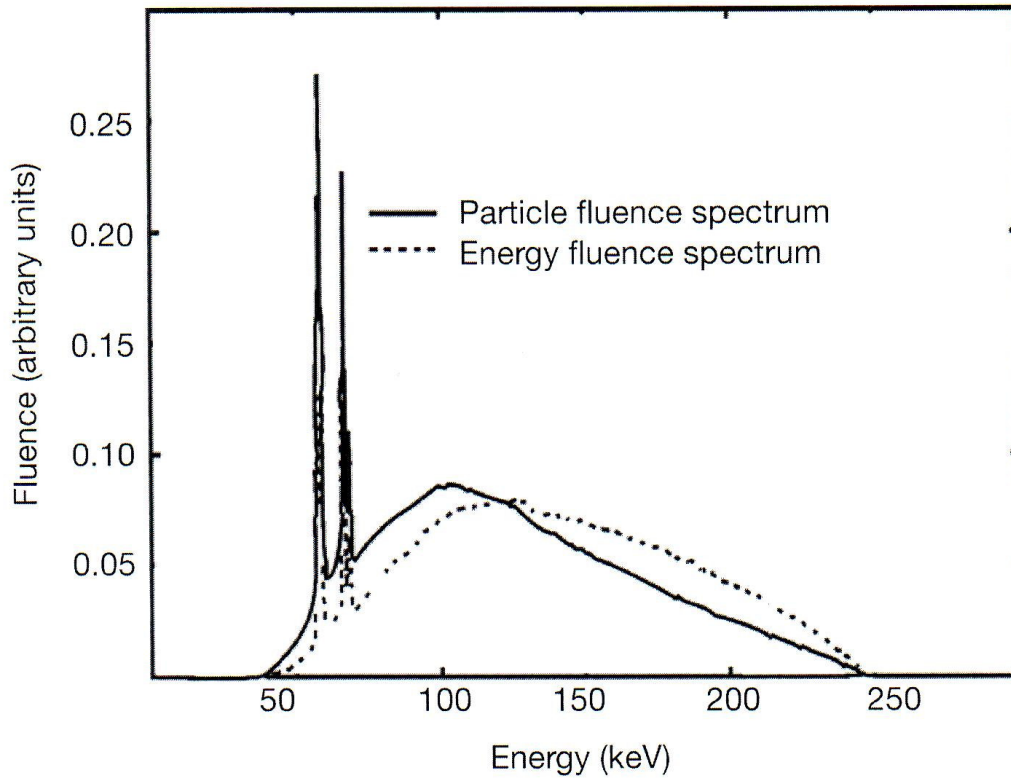


Figure A-1. Photon fluence and energy fluence spectra at 1 m from the target of an X-ray machine with a tube potential of 250 kV and added filtration of 1 mm Al and 1.8 mm Cu (target material: W; inherent filtration: 2 mm Be).⁹

A.3. KERMA

Kerma is an acronym for kinetic energy released per unit mass. It is a nonstochastic quantity applicable to indirectly ionizing radiation such as photons and neutrons. It quantifies the average amount of energy transferred from indirectly ionizing radiation to directly ionizing radiation without concern as to what happens after this transfer.⁹ The discussion that follows will be limited to photons. The energy of photons is imparted to matter in a two-stage process. In the first stage, the photon radiation transfers energy to the secondary charged particles (electrons) through various photon interactions (the photoelectric effect, the Compton Effect, pair production, etc.). In the second stage, the charged particle transfers energy to the medium through atomic excitations and ionizations. In this context, the kerma is defined as the mean energy transferred from the indirectly ionizing radiation to charged particles (electrons) in the medium $d\bar{E}_{tr}$ per unit mass dm :

$$K = \frac{d\bar{E}_{tr}}{dm} \quad (\text{A.3.1})$$

The unit of kerma is joule per kilogram (J/kg). The name for the unit of kerma is the gray (Gy), where $1 \text{ Gy} = 1 \text{ J/kg}$.⁹

A.3.1 Theoretical basis for the new air kerma based code

In the case of low- and medium-energy x-rays the determination of the absorbed dose is based on treating the measuring instrument as an exposure meter, by making use of the following general expression:

$$D_w = X \left(\frac{W}{e} \right) \left(\frac{\bar{\mu}_{en}}{e} \right)_{w/air} \quad (\text{A.3.2})$$

Where

D_w is the absorbed dose to water,

X is the exposure at the point at which the dose is required,

W/e is the quotient of the average energy expended to produce an ion pair in air by

the electronic charge and $\left(\frac{\bar{\mu}_{en}}{\rho} \right)_{w/air}$ is the ratio of mass energy absorption

coefficients of water to air averaged over the photon spectrum at the point of measurement¹⁵. This is in contrast to the use of Bragg-Gray Cavity theory used at megavoltage energies³. Air-kerma has replaced exposure as the preferred quantity.

The air kerma K_{air} is related to X by

$$K_{air} = X \left(\frac{W}{e} \right) \left(\frac{1}{1-g} \right) \quad (\text{A.3.3})$$

Where g is the fraction of energy of secondary charged particles lost to bremsstrahlung in air. At kilovoltage energies, it is assumed that

1. $g = 0$; therefore $\mu_{tr} = \mu_{en}$ and $K = K_{col}$, where μ_{tr} and μ_{en} are the energy transfer and energy absorption coefficients respectively, K is the kerma and K_{col} is the collision kerma, and
2. there is charged particle equilibrium at any position of measurement in the water phantom; therefore $D_w = K_{col,w}$.

Equation 3.3.2 expressed in terms air kerma then becomes

$$D_w = K_{air} \left(\frac{\bar{\mu}_{en}}{\rho} \right)_{w/air} \quad (\text{A.3.4})$$

The air kerma has to be determined at the point of interest in the beam by means of a calibrated ionisation chamber utilizing the following relationship:

$$K_{air} = MN_K \quad (\text{A.3.5})$$

where N_K is the air kerma calibration factor for the chamber free in air, at the particular HVL in question used to convert its response M , to air kerma at the point corresponding to the centre of the chamber in the absence of the chamber, under standard ambient conditions.

A.3.2 Medium-energy x-rays (0.5 mm Cu-4 mm Cu)

The recommendation is that dose determination is performed with the calibrated ionization chamber placed with its centre at depth of 2 cm in a water phantom^{8, 10}. It is assumed that any waterproof sheath is water equivalent. The response then corresponds to the air kerma at the centre of a hole in the phantom, with a shape equal to the outer dimensions of the chamber, providing that the photon fluence of the radiation field is identical to that during the in-air calibration. The influence of

changes in the energy and angular distribution of the photons incident on the surface of the ‘hole’ compared to free in-air, on the chamber’s response, are corrected by the factor k_Q defined thus:

$$K_{air,hole} = MN_K k_Q \quad (A.3.6)$$

A.3.2.1 Air kerma at the chamber centre in the undisturbed medium

The quantity that is ultimately required is the air kerma at the centre of the hole when it is filled with water. Thus a further correction is required to account for the effect on the chamber signal of replacing the disturbed phantom material. The two competing effects of over-reading due to lack of attenuation and under-reading due to lack of scatter are combined in the perturbation factor p_{dis} thus:

$$K_{air,z} = MN_K k_Q p_{dis} \quad (A.3.7)$$

where $K_{air,z}$ is the air kerma at the position of the chamber centre (at depth of 2 cm) in the undisturbed medium.

A.3.2.2 Correction for the effect of the chamber stem

Thus far no explicit account has been taken of the effect of the chamber stem. In fact, it is possible to treat this conceptually as simply part of the chamber wall. In practice, theoretical investigations of the displacement factor have been carried out for a stemless chamber. Then it becomes necessary to explicitly correct for the chamber stem. A global stem correction factor, $k_{stem,global}$ and the factors $k'_Q p'_{dis}$ for a stemless chamber¹¹:

$$k_Q p_{dis} = k'_Q p'_{dis} k_{stem,global} \quad (A.3.8)$$

It should be noted that the stem effect in the water phantom is responsible for the field size dependence of the overall correction factor Rosser⁶.

A.3.2.3 Air kerma to water kerma conversion

The remaining step is to convert from air kerma to water kerma at the reference depth. This is affected by multiplying by the water-to-air mass energy absorption coefficient ratio, evaluated for the photon spectrum present at the particular depth and the field size concerned:

$$K_{w,z} = K_{air,z} \left[\left(\frac{\bar{\mu}_{en}}{\rho} \right)_{w/air} \right]_{z=2,\phi} \quad (\text{A.3.9})$$

A.3.2.4 Absorbed dose at depth in phantom

Equating $K_{w,z=2}$ with $D_{w,z=2}$ yields, finally

$$D_{w,z=2} = MN_K k_Q p_{dis} \left[\left(\frac{\bar{\mu}_{en}}{\rho} \right)_{w/air} \right]_{z=2,\phi} \quad (\text{A.3.10})$$

A.3.3 Low-energy x-ray beams

For low energy beam, dose determination is performed with the field chamber free in-air. The instrument reading, corrected for temperature, pressure and ion recombination, yields a value for air kerma, free in air, $K_{air,air}$, according to equation A.3.5. The descriptor air pertains to quantities free in air¹⁰.

A.3.3.1 Water to air

The air kerma, free in air, $K_{air,air}$, is converted into water kerma, free in air, $K_{w,air}$, by multiplying by the water-to-air mass-energy absorption coefficient ratio for HVL in question.

$$K_{w,air} = K_{air,air} \left[\left(\frac{\bar{\mu}_{en}}{\rho} \right)_{w/air} \right]_{air} \quad (\text{A.3.11})$$

where $\left(\frac{\bar{\mu}_{en}}{\rho} \right)_{w/air}$ is averaged over the photon energy spectrum in air.

A.3.3.2 Water kerma at the phantom surface

The water kerma free in air $K_{w,air}$ is converted to water kerma at the surface of the water phantom $K_{w,z=0}$ by multiplying by the backscatter factor B_w ; the subscript w indicates that B_w is a ratio of water kermas, defined by

$$B_w = \frac{K_{w,z=0}}{K_{w,air}} \quad (\text{A.3.12})$$

A.3.3.3 Absorbed dose at the phantom surface

Finally, the assumption made that the absorbed dose to water at the surface $D_{w,z=0}$, is equal to the water kerma $K_{w,z=0}$; which is justified in the case of low-energy x-rays. The final expression is

$$D_{w,z=0} = MN_K B_w \left[\left(\frac{\bar{\mu}_{en}}{\rho} \right)_{w/air} \right]_{air} \quad (\text{A.3.13})$$

It can be noted that the quantity $D_{w,z=0}$ is the dose at a very small depth, where charged particles are first established.¹⁰

A.4 ABSORBED DOSE

Absorbed dose is a non-stochastic quantity applicable to both indirectly and directly ionizing radiations. For indirectly ionizing radiations, energy is imparted to matter in a two-step process. In the first step (resulting in kerma), the indirectly ionizing radiation transfers energy as kinetic energy to secondary charged particles. In the second step, these charged particles transfer some of their kinetic energy to the medium (resulting in absorbed dose) and lose some of their energy in the form of radiative losses (bremsstrahlung, annihilation in flight).⁹ The absorbed dose is related to the stochastic quantity energy imparted. The absorbed dose is defined as the mean energy $\bar{\mathcal{E}}$ imparted by ionizing radiation to matter of mass m in a finite volume V by:

$$D = \frac{d\bar{\mathcal{E}}}{dm} \quad (\text{A.4.9})$$

The energy imparted $\bar{\mathcal{E}}$ is the sum of all the energy entering the volume of interest minus all the energy leaving the volume, taking into account any mass–energy

conversion within the volume. Pair production, for example, decreases the energy by 1.022 MeV, while electron–positron annihilation increases the energy by the same amount. Note that because electrons travel in the medium and deposit energy along their tracks, this absorption of energy does not take place at the same location as the transfer of energy described by kerma. The unit of absorbed dose is joule per kilogram (J/kg). The name for the unit of absorbed dose is the gray (Gy).

A.5 DETERMINATION OF THE RATIO OF MASS-ENERGY ABSORPTION COEFFICIENT OF WATER TO AIR

The ratio of the mean mass-energy absorption coefficients of water to air is calculated using:

$$\left[\left(\frac{\bar{\mu}_{en}}{\rho} \right)_{w/a} \right]_{z=d,\phi} = \left(\int_0^E \frac{d\phi}{dE} \left(\frac{\mu_{en}}{\rho} \right)_w EdE \right) \left(\int_0^E \frac{d\phi}{dE} \left(\frac{\mu_{en}}{\rho} \right)_a EdE \right)^{-1} \quad (\text{A.5.10})$$

where $\frac{d\phi}{dE}$ is the photon fluence spectrum at a depth in water, $\left(\frac{\mu_{en}}{\rho} \right)_w$ is the monoenergetic value of the mass-energy absorption coefficient for water at energy E and $\left(\frac{\mu_{en}}{\rho} \right)_a$ is the monoenergetic value of the mass-energy absorption coefficient for air at energy E.⁶

8 . REFERENCES

1. Coosa Valley Technical College (CVTC)
http://test.cvtcollege.org/Ac_Programs/radtherapy/history.html
2. Jacob Van Dyk, The Modern Technology, A Compendium for Medical Physicists and Radiation Oncologists, Medical Physics Publishing, Madison, Wisconsin, 1999.
3. International Atomic Energy Agency (IAEA) 1987 Absorbed dose determination in photon and electron beams IAEA Technical Reports Series 277 (Vienna: IAEA).
4. British Journal of Radiology (BJR) 1996 Central axis depth dose data for use in radiotherapy Br.J.Radiol. Suppl 25.
5. FAIZ M. KHAN, Ph.D. The Physics of Radiation Therapy. William & Wilkins USA Second edition 1994.
6. K. E. Rosser An alternative beam quality index for medium-energy X-ray dosimetry National Physical Laboratory, Physics in Medicine & Biology 43 (1998).
7. J.R. Cunningham, University of Toronto; H.E. Johns, Ontario Cancer Institute and the Radiological Research Laboratories; University of Toronto. The Physics of Radiology, Fourth Edition, Charles C Thomas. Publisher, Springfield, Illinois, U.S.A., 1983.
8. AAPM's TG-61 protocol for 40-300 kV x-ray beam dosimetry in radiotherapy and radiobiology. Med. Phys. 28 (6), 2001.

9. Andreo, P., Evans, M.D.C., Hendry, J.H., Horton, J.L., Izewska, J, Mijnheer, B.J., Mills, J.A., Olivares, M., Ortiz López, P., Parker, W., Patrocinio, H., Podgorsak, E.B., Podgorsak, M.B., Rajan, G., Seuntjens, J.P., Shortt, K.R., Strydom, W., Suntharalingam, N., Thwaites, D.I., Tolli, H. RADIATION ONCOLOGY PHYSICS: A HANDBOOK FOR TEACHERS AND STUDENTS, INTERNATIONAL ATOMIC ENERGY AGENCY VIENNA, 2005

10. IPEMB 1996 The IPEMB code of practice for the determination of absorbed dose for x-rays below 300 kV generating potential (0.035 mm Al-4 mm Cu HVL; 10-300 kV generating potential) Phys. Med. Biol. **41** 2605-25.

11. International Atomic Energy Agency (IAEA) 1997 Absorbed dose determination in photon and electron beams, an International Code of Practice. 2ND edition, Technical Report Series 277 VIENNA, 1997.

12. IAEA TRS-398, Dosimetry and Medical Radiation Physics Section International Atomic Energy Agency, Absorbed dose to water determination in external beam radiotherapy: An international Code of practice for dosimetry based on standards of absorbed dose to water, IAEA, VIENNA, 2000.

13. IPEM Working Party: R J Aukett (Chair), J E Burns, A G Greener, R M Harrison, C Moretti, A E Nahum and K E Rosser, Institute of Physics and Engineering in Medicine, Fairmount House, 230 Tadcaster Road, York YO24 1ES, UK; Addendum to the IPEMB code of practice for the determination of absorbed dose for x-rays below 300 kV generating potential (0.035 mm Al-4 mm Cu HVL). Phys. Med. Biol. **50** (2005) 2739-2748.

14. Alan E. Nahum, Joint Department of Physics, Royal Marsden NHS Trust and Institute of Cancer Research, Sutton SM2 5PT, United Kingdom. kV X-ray Dosimetry: Current Status and Future Challenges, Medical Physics Publishing, Madison, WI, 1999.

15. International Commission on Radiation Units and Measurements (ICRU) 23
1973 Measurement of absorbed dose in a phantom irradiated by a single beam
of X or gamma rays ICRU Report 23 (Bethesda, MD: ICRU)
16. R. M. Harrison, Low energy X-ray depth dose data for use in radiotherapy-
comments on the review of BJR Supplement 17. *The British Journal of
Radiology*, 70 (1997).
17. C. K. Bomford, I. H. Kunkler, Walter and Miller's Textbook of Radiotherapy,
Radiation Physics, Therapy and Oncology. Churchill Livingstone, Elsevier
Science Limited, 2003.
18. AAPM's TG-51 protocol for clinical reference dosimetry of high-energy
photon and electron beams. *Med. Phys.* 28 (9), 1999.
19. Joseph C. Poen, M.D. Department of Radiation Oncology, Stanford
University, Stanford, CA USA, Clinical Application of Orthovoltage
Radiotherapy: Tumors of the Skin, Endorectal Therapy, and Intraoperative
Radiation Therapy, Medical Physics Publishing , 1999.
20. C. -M. Ma, C. W. Coffey, L. A De Werd, C. Liu, R. Nath, S. M. Seltzer and J.
Seuntjens, Ionizing Radiation Standards, National Research Council of
Canada, Ottawa, Canada K1A 0R6, Radiation Oncology Department,
Vanderbilt Medical Center, Nashville, TN 37232, Radiation Calibration Labs,
University of Wisconsin, Madison, WI 53706, Radiation Oncology
Department, University of Florida, Gainesville, FL 32610, Therapeutic
Radiology Department, Yale University School of Medicine, New Haven, CT
06510, Division of Ionizing Radiation, National Institute of Standards and
Technology (NIST), Gaithersburg, MD 20899. Status of Kilovoltage X-ray
Beam Dosimetry in Radiotherapy, Medical Physics Publishing, 1999.

21. C-M Ma and A. E. Nahum. Calculations of ion chamber displacement effect corrections for medium-energy X-ray dosimetry. *Phys. Med. Biol.* **40** (1995) 45-62.

22. Knight R T and Nahum A E 1994 Depth and field size dependence of ratios of mass energy absorption coefficient, water-to-air, for kV x-ray dosimetry *Proc. IAEA Int. Symp. on Measurement Assurance in Dosimetry (Vienna 1993)* IAEA-SM-330/17 (Vienna: IAEA) pp 361–70